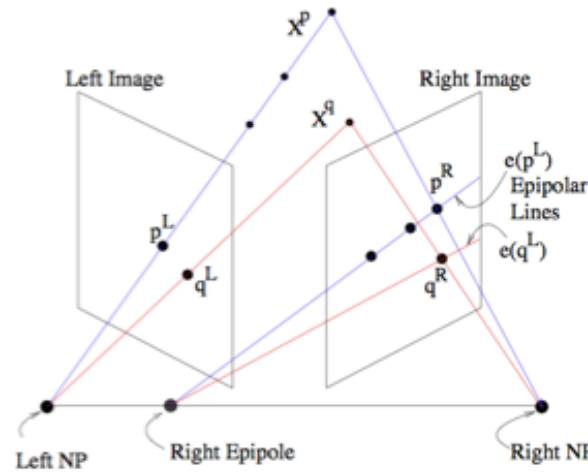


## Projection, stereo and panoramic images

$X^p$  and  $X^q$  are the physical location of objects.



<http://www.cs.toronto.edu/~jepson/csc420/notes/epiPolarGeom.pdf>  
(note, the image is posted on an educational site and copied here without following up on permissions. Any further use of the image should follow up on the origins and permissions.)

$(X_L)^T * F * X_R = 0$  for any pair of points in the images.

Note: the “Essential matrix” is a matrix used if the camera details are known. The “bifocal tensor”, a.k.a. “fundamental matrix” does not need camera details.

NP are the nadir points of the cameras.

The line connecting the left and right NP is the baseline.

The projection of the left nadir, NP is seen as the left epipole w.r.t. right image. The epipoles may or may not be within the border of the images.

The projection of  $X^p$  to left nadir, NP is seen as an epipole line in the right image. If more than one epipole line is present in the right image, they converge at the right epipole (which might not be within the boundaries of the image).

Once the points in the left image,  $X_L$  are matched with points in the right image,  $X_R$ , if there are at least 7 points, one can determine the “bifocal tensor”,  
a.k.a. “fundamental matrix, relating the points in the 2 images using a 3x3 matrix of rank 2.

### 9.2 The fundamental matrix F

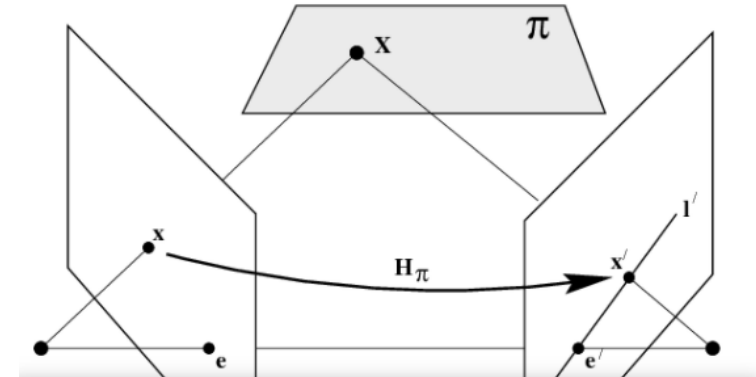


Fig. 9.5. A point  $x$  in one image is transferred via the plane  $\pi$  to a matching point  $x'$  in the second image. The epipolar line through  $x'$  is obtained by joining  $x'$  to the

## 2D transformations

from “Computer Vision: Algorithms and Applications” by Szeliski  
 (Note, please consult author and book for any use of this. it’s presented here for educational purposes only.)

**2D Translation.**  $x' = x + t$

$$x' = \begin{bmatrix} I & t \end{bmatrix} \bar{x}$$

$$\bar{x}' = \begin{bmatrix} I & t \\ 0^T & 1 \end{bmatrix} \bar{x}$$

where  $I$  is the  $(2 \times 2)$  identity matrix

**2D Affine:**  $x' = Ax^-$

$$x' = \begin{bmatrix} a_{00} & a_{01} & a_{02} \\ a_{10} & a_{11} & a_{12} \end{bmatrix} \bar{x}.$$

preserves parallel property of lines.

**2D Projective (a.k.a. perspective transformation, homography):**  $\tilde{x}' = \tilde{H}x'$

Note that  $\tilde{H}$  is homogeneous, i.e., it is only defined up to a scale.  
 Two  $H$  matrices that differ only by scale are equivalent.

The resulting homogeneous coordinate  $x'$  must be normalized in order to obtain an inhomogeneous result:

$$x' = \frac{h_{00}x + h_{01}y + h_{02}}{h_{20}x + h_{21}y + h_{22}} \text{ and } y' = \frac{h_{10}x + h_{11}y + h_{12}}{h_{20}x + h_{21}y + h_{22}}$$

preserves straightness property of lines.

**2D Rotation + translation (a.k.a. rigid body motion, a.k.a. 2D euclidian):**

$$x' = Rx + t$$

$$x' = \begin{bmatrix} R & t \end{bmatrix} \bar{x} \quad R = \begin{bmatrix} \cos \theta & -\sin \theta \\ \sin \theta & \cos \theta \end{bmatrix}$$

**2D Scaled rotation (a.k.a. similarity transform):**  $x' = sRx + t$

$$x' = \begin{bmatrix} sR & t \end{bmatrix} \bar{x} = \begin{bmatrix} a & -b & t_x \\ b & a & t_y \end{bmatrix} \bar{x}$$

preserves angles between lines.

Transformation	Matrix	# DoF	Preserves	Icon
translation	$[I   t]_{2 \times 3}$	2	orientation	
rigid (Euclidean)	$[R   t]_{2 \times 3}$	3	lengths	
similarity	$[sR   t]_{2 \times 3}$	4	angles	
affine	$[A]_{2 \times 3}$	6	parallelism	
projective	$[\tilde{H}]_{3 \times 3}$	8	straight lines	

**Table 2.1** Hierarchy of 2D coordinate transformations. Each transformation also preserves the properties listed in the rows below it, i.e., similarity preserves not only angles but also parallelism and straight lines. The  $2 \times 3$  matrices are extended with a third  $[0^T 1]$  row to form a full  $3 \times 3$  matrix for homogeneous coordinate transformations.

**Planar surface flow: Bilinear interpolant:**

$$x' = a_0 + a_1x + a_2y + a_6x^2 + a_7xy$$

$$y' = a_3 + a_4x + a_5y + a_7x^2 + a_6xy$$

planar surface with a small 3D motion

**Bilinear interpolant:**

$$x' = a_0 + a_1x + a_2y + a_6xy$$

$$y' = a_3 + a_4x + a_5y + a_7xy$$

useful for interpolation of sparse grids using splines , but does not preserve straight lines

## 3D transformations

from “Computer Vision: Algorithms and Applications” by Szeliski  
 (Note, please consult author and book for any use of this. it’s presented here for educational purposes only.)

**3D Translation.**  $\mathbf{x}' = \mathbf{x} + \mathbf{t}$

$$\mathbf{x}' = \begin{bmatrix} \mathbf{I} & \mathbf{t} \end{bmatrix} \bar{\mathbf{x}}$$

where  $\mathbf{I}$  is the  $(3 \times 3)$  identity matrix

**3D Affine:**  $\mathbf{x}' = \mathbf{A}\mathbf{x}^+$

$$\mathbf{x}' = \begin{bmatrix} a_{00} & a_{01} & a_{02} & a_{03} \\ a_{10} & a_{11} & a_{12} & a_{13} \\ a_{20} & a_{21} & a_{22} & a_{23} \end{bmatrix} \bar{\mathbf{x}}$$

preserves parallel property of lines and planes.

**3D Projective (a.k.a. perspective transformation, homography):**  $\tilde{\mathbf{x}}' = \tilde{\mathbf{H}}\tilde{\mathbf{x}}$

Note that  $\tilde{\mathbf{H}}$  is homogeneous, i.e., it is only defined up to a scale, Two  $\mathbf{H}$  matrices that differ only by scale are equivalent.

The resulting homogeneous coordinate  $\tilde{\mathbf{x}}'$  must be normalized in order to obtain an inhomogeneous result:

preserves straightness property of lines.

**3D Rotation + translation (a.k.a. rigid body motion, a.k.a. 3D euclidian):**  $\mathbf{x}' = \mathbf{R}\mathbf{x} + \mathbf{t}$

$$\mathbf{x}' = \begin{bmatrix} \mathbf{R} & \mathbf{t} \end{bmatrix} \bar{\mathbf{x}}$$

where  $\mathbf{R}$  is a  $3 \times 3$  orthonormal rotation matrix with  $\mathbf{R}\mathbf{R}^T = \mathbf{I}$  and  $|\mathbf{R}| = 1$ .

can describe a rigid motion using

$$\mathbf{x}' = \mathbf{R}(\mathbf{x} - \mathbf{c}) = \mathbf{R}\mathbf{x} - \mathbf{R}\mathbf{c}$$

where  $\mathbf{c}$  is the center of rotation (often the camera center).

**3D Scaled rotation (a.k.a. similarity transform):**  $\mathbf{x}' = s\mathbf{R}\mathbf{x} + \mathbf{t}$

$$\mathbf{x}' = \begin{bmatrix} s\mathbf{R} & \mathbf{t} \end{bmatrix} \bar{\mathbf{x}} = \begin{bmatrix} a & -b & t_x \\ b & a & t_y \end{bmatrix} \bar{\mathbf{x}},$$

preserves angles between lines and planes.

Transformation	Matrix	# DoF	Preserves	Icon
translation	$\begin{bmatrix} \mathbf{I} & \mathbf{t} \end{bmatrix}_{3 \times 4}$	3	orientation	
rigid (Euclidean)	$\begin{bmatrix} \mathbf{R} & \mathbf{t} \end{bmatrix}_{3 \times 4}$	6	lengths	
similarity	$\begin{bmatrix} s\mathbf{R} & \mathbf{t} \end{bmatrix}_{3 \times 4}$	7	angles	
affine	$\begin{bmatrix} \mathbf{A} \end{bmatrix}_{3 \times 4}$	12	parallelism	
projective	$\begin{bmatrix} \tilde{\mathbf{H}} \end{bmatrix}_{4 \times 4}$	15	straight lines	

**Table 2.2** Hierarchy of 3D coordinate transformations. Each transformation also preserves the properties listed in the rows below it, i.e., similarity preserves not only angles but also parallelism and straight lines. The  $3 \times 4$  matrices are extended with a fourth  $[0^T \ 1]$  row to form a full  $4 \times 4$  matrix for homogeneous coordinate transformations. The mnemonic icons are drawn in 2D but are meant to suggest transformations occurring in a full 3D cube.

## 3D transformations

from “Computer Vision: Algorithms and Applications” by Szeliski  
 (Note, please consult author and book for any use of this. it’s presented here for educational purposes only.)

### 3D Rotation represented by a rotation axis and angle (a.k.a. Rodriguez’s formula).

rotation axis and angle as a vector  $\omega = \theta\hat{n}$

let  $[\hat{n}]$  be the matrix form of the cross product operator with the vector  $\hat{n} = (\hat{n}_x, \hat{n}_y, \hat{n}_z)$ ,

$$[\hat{n}]_x = \begin{bmatrix} 0 & -\hat{n}_z & \hat{n}_y \\ \hat{n}_z & 0 & -\hat{n}_x \\ -\hat{n}_y & \hat{n}_x & 0 \end{bmatrix}$$

and

$$\mathbf{R}(\hat{n}, \theta) = \mathbf{I} + \sin \theta [\hat{n}]_x + (1 - \cos \theta) [\hat{n}]_x^2$$

*good for small rotations*

For infinitesimal or instantaneous) rotations and  $\theta$  expressed in radians, Rodriguez’s formula simplifies to:

$$\mathbf{R}(\omega) \approx \mathbf{I} + \sin \theta [\hat{n}]_x \approx \mathbf{I} + [\theta \hat{n}]_x = \begin{bmatrix} 1 & -\omega_z & \omega_y \\ \omega_z & 1 & -\omega_x \\ -\omega_y & \omega_x & 1 \end{bmatrix}$$

from “Bundle Adjustment — A Modern Synthesis” by Triggs et al.:

Rotations should be parametrized using either quaternions subject to  $\|q\|^2 = 1$ , or local perturbations  $R\delta R$  or  $\delta R R$  of an existing rotation  $R$ , where  $\delta R$  can be any well-behaved 3 parameter small rotation approximation, e.g.  $\delta R = (\mathbf{I} + [\delta r]_x)$ , the Rodriguez formula, local Euler angles, etc.

**State updates:** Just as state vectors  $x$  represent points in some nonlinear space, state updates  $x \rightarrow x + \delta x$  represent displacements in this nonlinear space that often can not be represented exactly by vector addition.

## 3D transformations

from “Computer Vision: Algorithms and Applications” by Szeliski  
 (Note, please consult author and book for any use of this. it’s presented here for educational purposes only.)

### 3D Rotation represented Unit quaternions:

(Shoemake 1985)

a unit length 4-vector whose components can be written as

$$\mathbf{q} = (q_x, q_y, q_z, q_w) \text{ or } \mathbf{q} = (x, y, z, w)$$

Unit quaternions live on the unit sphere  $\|\mathbf{q}\| = 1$  and *antipodal* (opposite sign) quaternions,  $\mathbf{q}$  and  $-\mathbf{q}$ , represent the same rotation

^ “origin”  $\mathbf{q}_o = (0, 0, 0, 1)$ .

$$\mathbf{q} = (\mathbf{v}, w) = \left( \sin \frac{\theta}{2} \hat{\mathbf{n}}, \cos \frac{\theta}{2} \right),$$

to express Rodriguez’s formula:

$$\begin{aligned} \mathbf{R}(\hat{\mathbf{n}}, \theta) &= \mathbf{I} + \sin \theta [\hat{\mathbf{n}}]_{\times} + (1 - \cos \theta) [\hat{\mathbf{n}}]_{\times}^2 \\ &= \mathbf{I} + 2w[\mathbf{v}]_{\times} + 2[\mathbf{v}]_{\times}^2. \end{aligned}$$

$$\mathbf{R}(\mathbf{q}) = \begin{bmatrix} 1 - 2(y^2 + z^2) & 2(xy - zw) & 2(xz + yw) \\ 2(xy + zw) & 1 - 2(x^2 + z^2) & 2(yz - xw) \\ 2(xz - yw) & 2(yz + xw) & 1 - 2(x^2 + y^2) \end{bmatrix}. \quad (2.41)$$

The diagonal terms can be made more symmetrical by replacing  $1 - 2(y^2 + z^2)$  with  $(x^2 + w^2 - y^2 - z^2)$ , etc.

Given two quaternions  $\mathbf{q}_0 = (v_0, w_0)$  and  $\mathbf{q}_1 = (v_1, w_1)$ ,

the *quaternion multiply* operator is defined as:

$$\mathbf{q}_2 = \mathbf{q}_0 \mathbf{q}_1 = (\mathbf{v}_0 \times \mathbf{v}_1 + w_0 \mathbf{v}_1 + w_1 \mathbf{v}_0, w_0 w_1 - \mathbf{v}_0 \cdot \mathbf{v}_1).$$

quaternion division:

$$\mathbf{q}_2 = \mathbf{q}_0 / \mathbf{q}_1 = \mathbf{q}_0 \mathbf{q}_1^{-1} = (\mathbf{v}_0 \times \mathbf{v}_1 + w_0 \mathbf{v}_1 - w_1 \mathbf{v}_0, -w_0 w_1 - \mathbf{v}_0 \cdot \mathbf{v}_1).$$

good for tracking of a smoothly moving camera, since there are no discontinuities in the representation. It is also easier to interpolate between rotations and to chain rigid transformations (Murray, Li, and Sastry 1994; Bregler and Malik 1998).

can use quaternions, and update estimates using an incremental rotation, as described in Section 6.2.2

## 3D → 2D Perspective Projection

$$\begin{bmatrix} X_c \\ Y_c \\ Z_c \end{bmatrix} = [\mathbf{R}]_{3 \times 3} \begin{bmatrix} X \\ Y \\ Z \end{bmatrix} + \mathbf{t}$$

$$\begin{bmatrix} u \\ v \\ 1 \end{bmatrix} \sim \begin{bmatrix} U \\ V \\ W \end{bmatrix} = \begin{bmatrix} f & 0 & u_c \\ 0 & f & v_c \\ 0 & 0 & 1 \end{bmatrix} \begin{bmatrix} X_c \\ Y_c \\ Z_c \end{bmatrix}$$

Richard Szeliski

Image Stitching

29

## Homogeneous coordinates

Is this a linear transformation?

- no—division by  $z$  is nonlinear

Trick: add one more coordinate:

$$(x, y) \Rightarrow \begin{bmatrix} x \\ y \\ 1 \end{bmatrix} \quad (x, y, z) \Rightarrow \begin{bmatrix} x \\ y \\ z \\ 1 \end{bmatrix}$$

homogeneous image coordinates      homogeneous scene coordinates

Converting from homogeneous coordinates

$$\begin{bmatrix} x \\ y \\ w \end{bmatrix} \Rightarrow (x/w, y/w) \quad \begin{bmatrix} x \\ y \\ z \\ w \end{bmatrix} \Rightarrow (x/w, y/w, z/w)$$

## Perspective Projection

Projection is a matrix multiply using homogeneous coordinates:

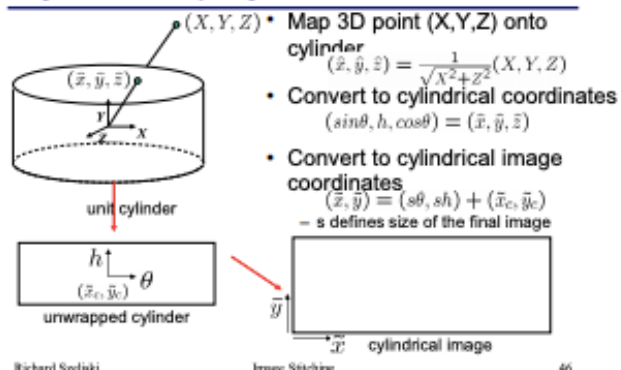
$$\begin{bmatrix} 1 & 0 & 0 & 0 \\ 0 & 1 & 0 & 0 \\ 0 & 0 & -1/d & 0 \end{bmatrix} \begin{bmatrix} x \\ y \\ z \\ 1 \end{bmatrix} = \begin{bmatrix} x \\ y \\ z \\ 1 \end{bmatrix} \Rightarrow \left( -d\frac{x}{z}, -d\frac{y}{z} \right)$$

divide by third coordinate

This is known as **perspective projection**

- The matrix is the **projection matrix**

## Cylindrical projection



Richard Szeliski

Image Stitching

46

## Global alignment

- Register **all** pairwise overlapping images
- Use a 3D rotation model (one R per image)
- Use direct alignment (patch centers) or feature based
- Infer overlaps based on previous matches (incremental)
- Optionally discover which images overlap other images using feature selection (RANSAC)

Richard Szeliski

Image Stitching

75

## Degrees of Freedom (DOF)

Similarity Transformation in 2D space:

4 DOF: 2 for translation, 1 for rotation, 1 for scale

Affine Transformation in 2D space:

6 DOF: 2 for translation, 1 for rotation, 1 for scale, 1 for aspect ratio, 1 for shear

Cartesian 3D space:

6 DOF (three for position and three for orientation)

Rigid Body in D-dimensional space:

translational: d

rotational:  $d*(d-1)/2$

Projective Transformation (homogenous coordinates):

8 DOF: 2 for translation, 1 for rotation, 1 for scale, 1 distortion of x for depth, 1 distortion of y for depth

Rotation in 3D space:

$$R_{z,\theta} = \begin{vmatrix} \cos(\theta) & -\sin(\theta) & 0 \\ \sin(\theta) & \cos(\theta) & 0 \\ 0 & 0 & 1 \end{vmatrix} \quad R_{x,\theta} = \begin{vmatrix} 1 & 0 & 0 \\ 0 & \cos(\theta) & -\sin(\theta) \\ 0 & \sin(\theta) & \cos(\theta) \end{vmatrix} \quad R_{y,\theta} = \begin{vmatrix} \cos(\theta) & 0 & \sin(\theta) \\ 0 & 1 & 0 \\ -\sin(\theta) & 0 & \cos(\theta) \end{vmatrix}$$

	1 View Known Structure	2 Views Unknown Structure	$n > 2$ Views Unknown Structure
Known intrinsics	Unique	Two-fold or unique	Unique
Unknown fixed focal length	Unique in general	1 d.o.f.	Unique in general
Unknown variable intrinsics	3 d.o.f.	2 d.o.f.	3n-4 d.o.f.

D. Nister. An efficient solution to the five-point relative pose problem. In Proc. 2003 IEEE Computer Society Conference on Computer Vision and Pattern Recognition(CVPR'03), volume 2, pages 195–202, June 2003

Table 1: The degrees of ambiguity in the face of planar degeneracy for pose estimation and structure and motion estimation. The motion is assumed to be general and the structure is assumed to be dense in the plane. See the text for further explanation.

## The Camera Matrix

from “Refinement in 3D Reconstruction using Cheirality Constraints” by Sengupta and Das” (<https://pdfs.semanticscholar.org/b603/af27e5e72352ab75782e4b07f5f2aa669a57.pdf>)

The Camera matrix contains the information of the camera; both the internal parameters, namely the zoom, focus, skew and external parameters like rotation and the translation with respect to the world coordinate frame. The camera matrix is given as P.

$$P = K[R|t]$$

where, K contains the camera internal parameters, R and t are rotation and translation parameters.. The internal parameters are arranged in an upper-triangular matrix,

$$K = \begin{bmatrix} \alpha_x & s & x_0 \\ & \alpha_y & y_0 \\ & & 1 \end{bmatrix}$$

where  $\alpha_x$  and  $\alpha_y$  represent the focal length in terms of pixel dimension in the x and y direction respectively, s is the camera skew and  $(x_0, y_0)^T$  are the coordinates of the principal point.

Cheirality constraints arise from the fact that any point that lies in an image must lie in front of the camera producing that image. The depth of a point  $X = [X, Y, Z, T]$ , with respect to the camera  $P = [M|I_m]$ , is given as

$$\text{depth}(X; P) = \frac{\text{sign}(\det M)w}{T\|\mathbf{m}^3\|}$$

$\text{sign}(\text{depth}(X; P))$  is known as the cheirality of point X with respect to camera P.

## Perspective Projection

from “Computer Vision: Algorithms and Applications” by Szeliski  
 (Note, please consult author and book for any use of this. it’s presented here for educational purposes only.)

points are projected unto an image plane by dividing them by their z-components, sometimes scaled between near and far clipping planes.

**for inhomogeneous and homogeneous coordinates, respectively:**

$$\bar{\mathbf{x}} = \mathcal{P}_z(\mathbf{p}) = \begin{bmatrix} x/z \\ y/z \\ 1 \end{bmatrix} \quad \tilde{\mathbf{x}} = \begin{bmatrix} 1 & 0 & 0 & 0 \\ 0 & 1 & 0 & 0 \\ 0 & 0 & 1 & 0 \end{bmatrix} \tilde{\mathbf{p}} \quad \tilde{\mathbf{x}} = \begin{bmatrix} 1 & 0 & 0 & 0 \\ 0 & 1 & 0 & 0 \\ 0 & 0 & -z_{\text{far}}/z_{\text{range}} & z_{\text{near}}z_{\text{far}}/z_{\text{range}} \\ 0 & 0 & 1 & 0 \end{bmatrix} \tilde{\mathbf{p}},$$

Note, cannot recover the distance to the 3D point after projection.

In comp graphics, projection is usually in 2-steps:

- 1) project 3D coordinates into *normalized device coordinates* in the range  $(x, y, z) \in [-1, -1] \times [-1, 1] \times [0, 1]$
- 2) rescale these coordinates to integer pixel coordinates using a *viewport* transformation

*disparity*, the inverse depth, is defined using  $z_{\text{near}} = 1$ ,  $z_{\text{far}} \rightarrow \infty$ , and switching the sign of the third row.

*distance* to a surface point can be measured using range sensors and stereo matching algorithms.

using that distance or the disparity, the 3D location can be estimated using inverse of a 4X4 matrix.

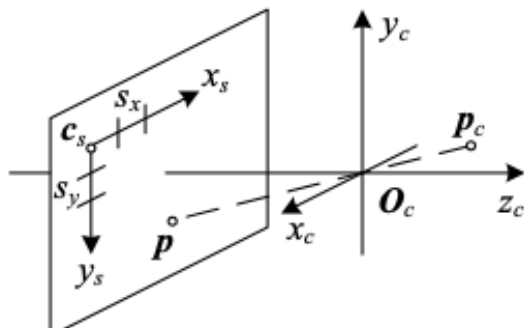


Fig 2.8 Projection of a 3D camera-centered point  $p_c$  onto the sensor planes at location  $p$ .  $O_c$  is the camera center (nodal point),  $c_s$  is the 3D origin of the sensor plane coordinate system, and  $s_x$  and  $s_y$  are the pixel spacings.

## Perspective Projection, camera matrices

from “Computer Vision: Algorithms and Applications” by Szeliski  
 (Note, please consult author and book for any use of this. it’s presented here for educational purposes only.)

points are projected unto an image plane by dividing them by their z-components, sometimes scaled between near and far clipping planes.

**for inhomogeneous and homogeneous coordinates, respectively:**

$$\mathbf{p} = \left[ \begin{array}{c|c} \mathbf{R}_s & \mathbf{c}_s \end{array} \right] \begin{bmatrix} s_x & 0 & 0 \\ 0 & s_y & 0 \\ 0 & 0 & 0 \\ 0 & 0 & 1 \end{bmatrix} \begin{bmatrix} x_s \\ y_s \\ 1 \end{bmatrix} = \mathbf{M}_s \bar{\mathbf{x}}_s$$

$$\tilde{\mathbf{x}}_s = \alpha \mathbf{M}_s^{-1} \mathbf{p}_c = \mathbf{K} \mathbf{p}_c$$

where  $\mathbf{M}_s$  is sensor homography. parameterized by 8 unknowns: the 3 parameters describing the rotation  $\mathbf{R}_s$ , the 3 parameters describing the translation  $\mathbf{c}_s$ , and the two scale factors ( $s_x, s_y$ ). often a 3X3 matrix is used

( $x_s, y_s$ ) are the pixel coordinates from the image sensor

( $s_x, s_y$ ) are the pixel spacings (e.g. in units of microns)

$\mathbf{O}_c$  is the camera projection center

$\mathbf{c}_s$  is the origin in  $\mathbf{O}_c$

$\mathbf{R}_s$  is the 3D rotation

$\mathbf{K}$  is the camera intrinsic matrix (a.k.a. the calibration matrix), which is used to map 3D camera-centered points  $\mathbf{p}_c$  to 2D pixel coordinates  $\tilde{\mathbf{x}}$ . It has 7 degrees of freedom, but 8 in practice.

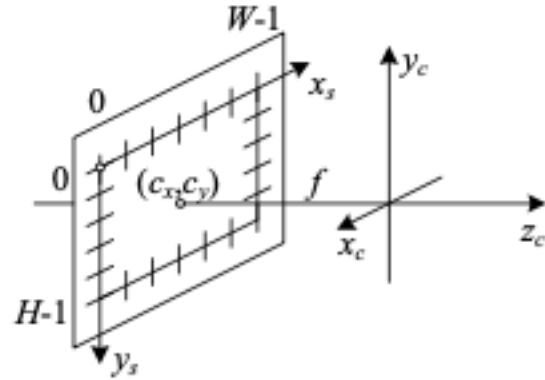
The camera’s orientation in space is called extrinsics (e.g. ( $\mathbf{R}, \mathbf{t}$ ))

NOTE that multi-view geometry in practice treats  $\mathbf{K}$  as an upper-left triangular matrix with 5 degrees of freedom.

## Perspective Projection, camera matrices

from “Computer Vision: Algorithms and Applications” by Szeliski  
 (Note, please consult author and book for any of this. use it's presented here for educational purposes only.)

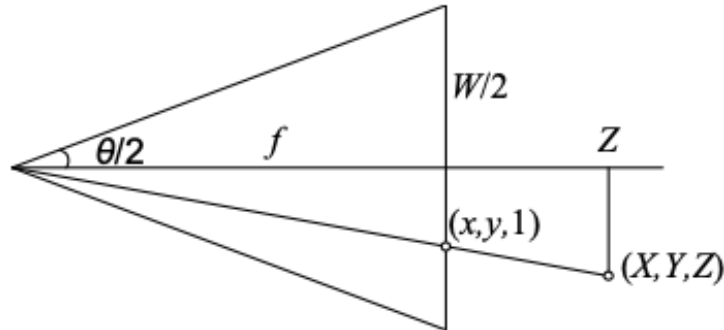
**Fig 2.9 Simplified camera intrinsics showing the focal length  $f$  and the optical center  $(c_x, c_y)$ . The image width and height are  $W$  and  $H$ .**



$$\mathbf{K} = \begin{bmatrix} f & s & c_x \\ 0 & af & c_y \\ 0 & 0 & 1 \end{bmatrix}$$

$(c_x, c_y)$  is the *optical center* in pixel coordinates

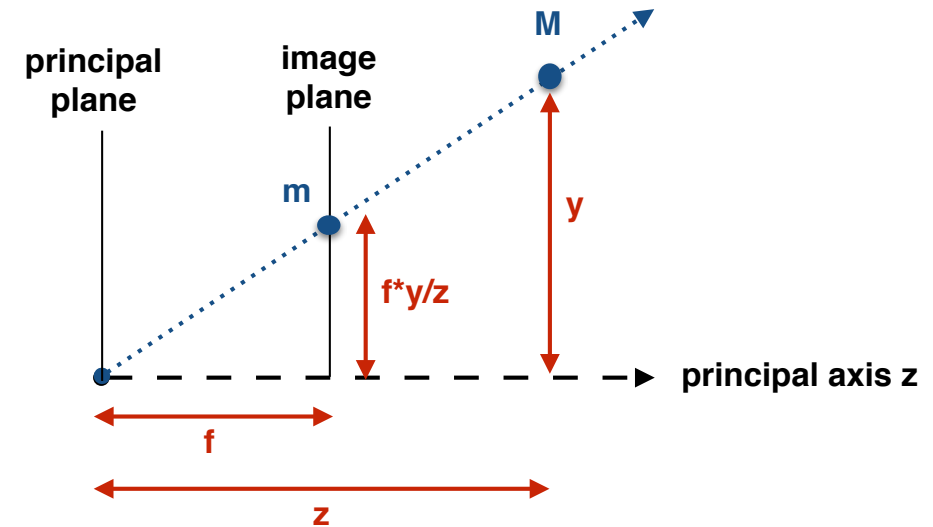
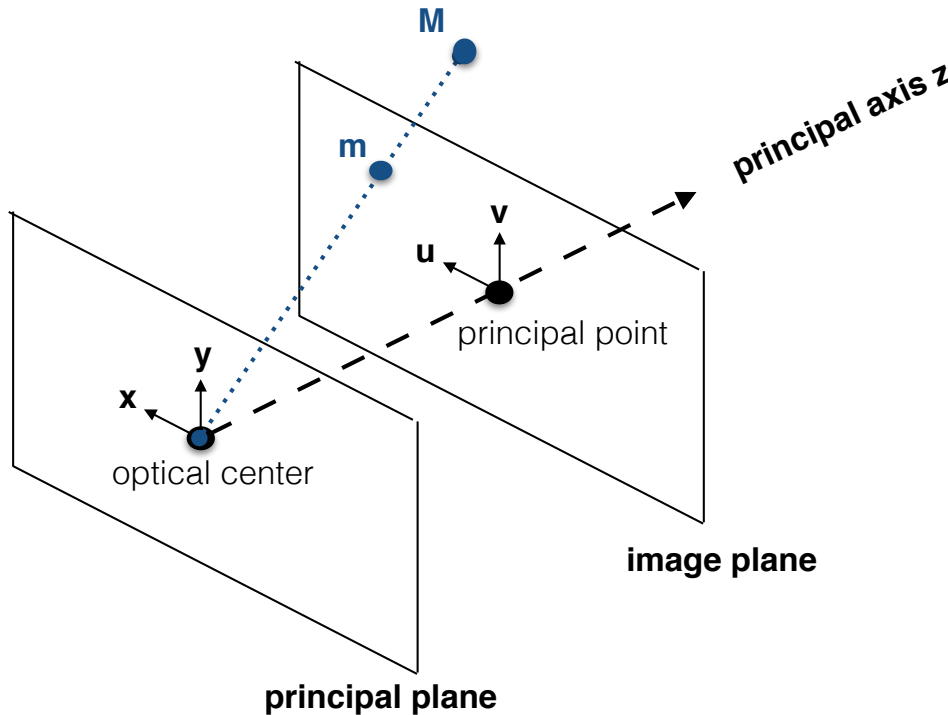
if set the origin at roughly the center of the image, e.g.,  $(cx, cy) = (W/2, H/2)$ , where  $W$  and  $H$  are the image height and width, the camera model has a single unknown, i.e., the focal length  $f$ .  $\theta$  is the FOV.  $f = (W/2)(\tan(\theta/2))^{-1}$



camera matrix

$$\mathbf{P} = \mathbf{K}[\mathbf{R}|\mathbf{t}]$$

## Pinhole camera geometry



camera projection matrix  $P$  is defined in  $z^* \mathbf{m} = P^* \mathbf{M}$   
 where  $\mathbf{M} = (x, y, z, 1)^T$  and  $\mathbf{m} = (f*x/z, f*y/z, 1)^T$

The right side of the projection eqn can be modified by rotation matrix  $\mathbf{R}$  and translation vector  $\mathbf{t}$  to put the coordinates in the (external) world coordinate system. The matrix is  $\begin{vmatrix} \mathbf{R} & \mathbf{t} \\ 0 & 1 \end{vmatrix}$   
 The six parameters are called *external parameters*.  
 rows of  $\mathbf{R}$  and the *optical center* describe the *camera reference frame* in world coordinates.

The left side of the projection eqn can be modified to change coordinates in the image frame.

$K = \begin{vmatrix} f/s_x & f/s_x * \cot\theta & o_x \\ 0 & f/s_y & o_y \\ 0 & 0 & 1 \end{vmatrix}$  *K* is the *camera calibration matrix*,  
 result is pixel coords in image plane.



## Pinhole camera geometry (cont.)

*intrinsic parameters:*

$f$  is the focal distance in mm

$o_x, o_y$  is the principal point in pixel coordinates

$s_x$  is the width of the pixel in mm

$s_y$  is the height of the pixel in mm

$\phi$  is the angle between the axes, usually 90 degrees

The aspect ratio  $s_x/s_y$  is usually 1

The *extrinsic parameters* depend upon Rotation and Translation of the camera.

$P$  can be rewritten as  $P = K^*[ I | 0 ]^*G = K^*[ R | t ]$

A scale factor  $\lambda$  applied is  $P = \lambda^*K^*[ R | t ]$

This is a 3x4 full rank matrix and can be factorized by QR factorization.

$P$  can be rewritten as  $P = [ P_{3x3} | p_4 ]$  where  $P_{3x3}$  is the first 3 rows of  $P$  and  $p_4$  is the 4th column.

If  $\lambda=1$ , the matrix is normalized and the distance of  $M$  from the focal plane of the camera is *depth*.

For the image plane at infinity, the image of points doesn't depend on camera position.

The angle between 2 rays is  $\cos \theta = m_1^T * \omega * m_2 / (\sqrt{m_1^T * \omega * m_1} * \sqrt{m_2^T * \omega * m_2})$

*extrinsic parameters* are the position and orientation of the camera w.r.t. a coord frame.

(Notes on pinhole camera followed by a few notes on multi-view geometry are from  
[http://homepages.inf.ed.ac.uk/rbf/CVonline/LOCAL\\_COPIES/FUSIELLO4/tutorial.html](http://homepages.inf.ed.ac.uk/rbf/CVonline/LOCAL_COPIES/FUSIELLO4/tutorial.html))



projection and the principal and image planes

remembering that the center of projection is in the principal plane one can define the position of m with respect to the 0,0 coordinates in the image plane in which it is in.

$u_c$  and  $v_c$  are the coordinates of the principal point.

m is at  $x, y$  in that image plane.

$$u = u_c + (x/\text{pixelWidth}) \quad \text{and} \quad v = v_c + (y/\text{pixelHeight})$$

Similarly, the coordinates in the world coordinate system can be transformed to the image plane coordinate system.

$$Z^*u = Z^*u_c + (X * f)/\text{pixelWidth}$$

$$Z^*v = Z^*v_c + (Y * f)/\text{pixelHeight}$$

using scaling factor:

$$\begin{vmatrix} |scale * u| & |(f/pixelWidth) & 0 & u_c & 0 | & } X | \\ |scale * v| & |0 & (f/pixelHeight) & v_c & 0 | & } Y | \\ | scale | & |0 & 0 & 1 & 0 | & } Z | \\ & & & & | 1 | \end{vmatrix}$$

camera calibration matrix:

$$C = \begin{vmatrix} |r_1 * (f/pixelWidth) + u_c * r_3 & t_x * (f/pixelWidth) + u_c * t_z | \\ |r_2 * (f/pixelHeight) + v_c * r_3 & t_y * (f/pixelHeight) + v_c * t_z | \\ |r_3 & t_z| \end{vmatrix}$$

# 3D transformations

from “Computer Vision: Algorithms and Applications” by Szeliski

(Note, please consult author and book for any use of this. it’s presented here for educational purposes only.)

Transformation	Matrix	# DoF	Preserves	Icon
translation	$\begin{bmatrix} \mathbf{I} & \mathbf{t} \end{bmatrix}_{2 \times 3}$	2	orientation	
rigid (Euclidean)	$\begin{bmatrix} \mathbf{R} & \mathbf{t} \end{bmatrix}_{2 \times 3}$	3	lengths	
similarity	$\begin{bmatrix} s\mathbf{R} & \mathbf{t} \end{bmatrix}_{2 \times 3}$	4	angles	
affine	$\begin{bmatrix} \mathbf{A} \end{bmatrix}_{2 \times 3}$	6	parallelism	
projective	$\begin{bmatrix} \tilde{\mathbf{H}} \end{bmatrix}_{3 \times 3}$	8	straight lines	

**Table 2.1** Hierarchy of 2D coordinate transformations. Each transformation also preserves the properties listed in the rows below it, i.e., similarity preserves not only angles but also parallelism and straight lines. The  $2 \times 3$  matrices are extended with a third  $[0^T \ 1]$  row to form a full  $3 \times 3$  matrix for homogeneous coordinate transformations.

Transform	Matrix	Parameters $p$	Jacobian $J$
translation	$\begin{bmatrix} 1 & 0 & t_x \\ 0 & 1 & t_y \end{bmatrix}$	$(t_x, t_y)$	$\begin{bmatrix} 1 & 0 \\ 0 & 1 \end{bmatrix}$
Euclidean	$\begin{bmatrix} c_\theta & -s_\theta & t_x \\ s_\theta & c_\theta & t_y \end{bmatrix}$	$(t_x, t_y, \theta)$	$\begin{bmatrix} 1 & 0 & -s_\theta x - c_\theta y \\ 0 & 1 & c_\theta x - s_\theta y \end{bmatrix}$
similarity	$\begin{bmatrix} 1+a & -b & t_x \\ b & 1+a & t_y \end{bmatrix}$	$(t_x, t_y, a, b)$	$\begin{bmatrix} 1 & 0 & x & -y \\ 0 & 1 & y & x \end{bmatrix}$
affine	$\begin{bmatrix} 1+a_{00} & a_{01} & t_x \\ a_{10} & 1+a_{11} & t_y \end{bmatrix}$	$(t_x, t_y, a_{00}, a_{01}, a_{10}, a_{11})$	$\begin{bmatrix} 1 & 0 & x & y & 0 & 0 \\ 0 & 1 & 0 & 0 & x & y \end{bmatrix}$
projective	$\begin{bmatrix} 1+h_{00} & h_{01} & h_{02} \\ h_{10} & 1+h_{11} & h_{12} \\ h_{20} & h_{21} & 1 \end{bmatrix}$	$(h_{00}, h_{01}, \dots, h_{21})$	(see Section 6.1.3)

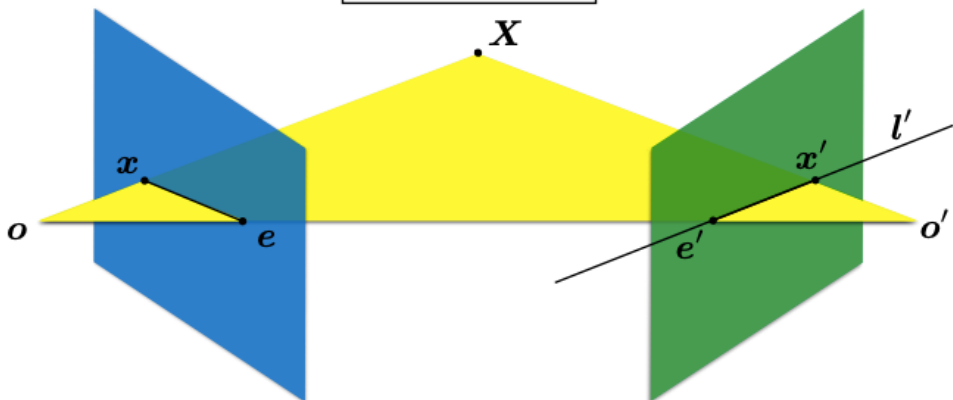
**Table 6.1** Jacobians of the 2D coordinate transformations  $\mathbf{x}' = \mathbf{f}(\mathbf{x}; \mathbf{p})$  shown in Table 2.1, where we have re-parameterized the motions so that they are identity for  $\mathbf{p} = 0$ .

## Points and Epipolar geometry: Essential Matrix

[http://www.cs.cmu.edu/~16385/s17/Slides/12.2\\_Essential\\_Matrix.pdf](http://www.cs.cmu.edu/~16385/s17/Slides/12.2_Essential_Matrix.pdf)

Given a point in one image, multiplying by the **essential matrix** will tell us the **epipolar line** in the second view.

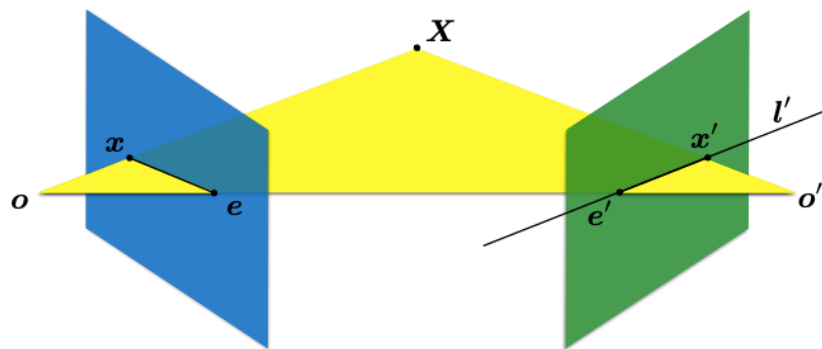
$$\mathbf{E}\mathbf{x} = \mathbf{l}'$$



**NOTE: o to o' is the baseline.**

So if  $\mathbf{x}^\top \mathbf{l} = 0$  and  $\mathbf{E}\mathbf{x} = \mathbf{l}'$  then

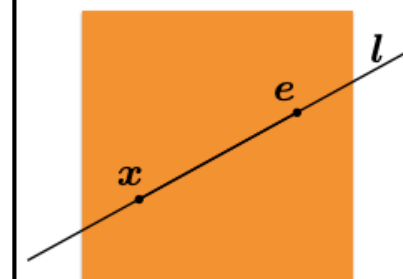
$$\mathbf{x}'^\top \mathbf{E}\mathbf{x} = 0$$



## Epipolar Line

$$ax + by + c = 0 \quad \text{in vector form}$$

$$\mathbf{l} = \begin{bmatrix} a \\ b \\ c \end{bmatrix}$$



If the point  $\mathbf{x}$  is on the epipolar line  $\mathbf{l}$  then

$$\mathbf{x}^\top \mathbf{l} = 0$$

<https://www.robots.ox.ac.uk/~vgg/hzbook/hzbook1/HZepipolar.pdf>

$e'$  is the **left null-space of F**.

Similarly  $Fe = 0$ , i.e.

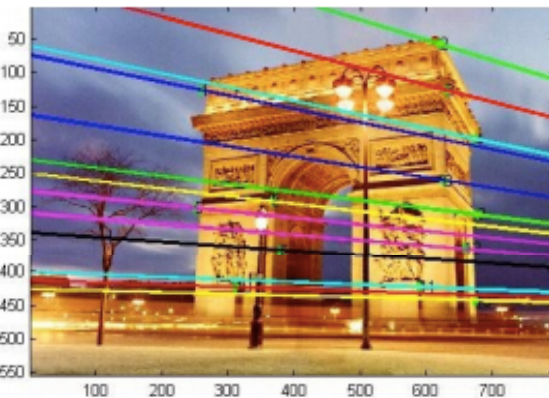
$e$  is the **right null-space of F**.

coords of epipole  $e'$  w.r.t. left image coords is where the right camera is w.r.t. left image coords=  $\text{svd}(F^T F).u[2]/\text{svd}(F^T F).u[2][2]$

## Points and Epipolar geometry: Essential Matrix

[http://www.cs.cmu.edu/~16385/s17/Slides/12.2\\_Essential\\_Matrix.pdf](http://www.cs.cmu.edu/~16385/s17/Slides/12.2_Essential_Matrix.pdf)

coords of right camera center in left image coords is epipole e =  
 $\text{svd}(F^T * F).u[2]/\text{svd}(F^T * F).u[2][2]$



epipole e

```
>> [u,d] = eigs(F' * F)
```

eigenvectors

```
u =
```

-0.0013	0.2586	-0.9660
0.0029	-0.9660	-0.2586
1.0000	0.0032	-0.0005

Eigenvector associated with  
smallest eigenvalue

```
>> uu = u(:,3)
```

( -0.9660	-0.2586	-0.0005 )
-----------	---------	-----------

eigenvalue

```
d = 1.0e8*
```

-1.0000	0	0
0	-0.0000	0
0	0	-0.0000

Epipole projected to image  
coordinates

```
>> uu / uu(3)
```

( 1861.02	498.21	1.0 )
-----------	--------	-------

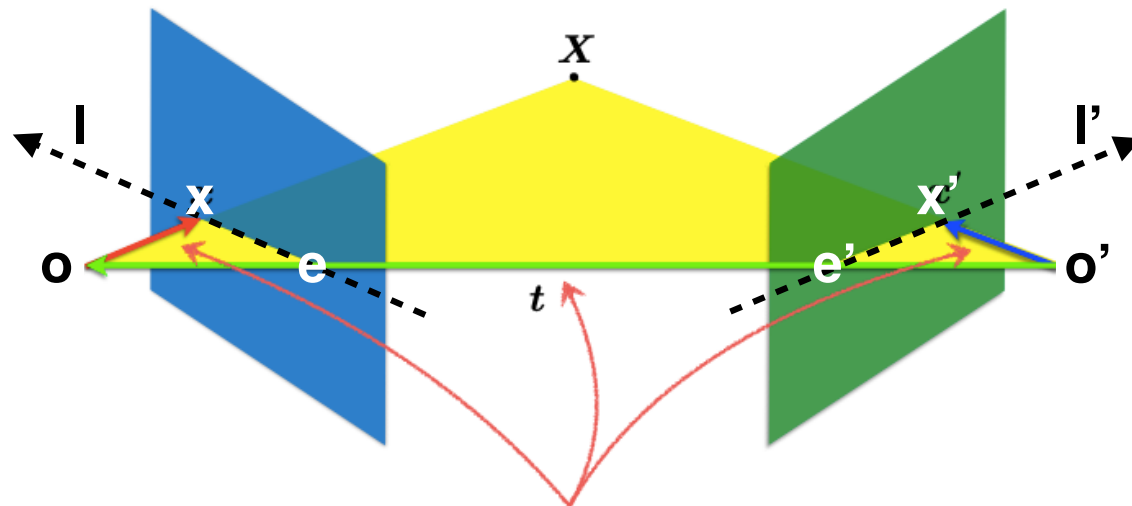
NOTE:

$\text{SVD}(A).U == \text{SVD}(AA^T).U == \text{SVD}(AA^T).V$

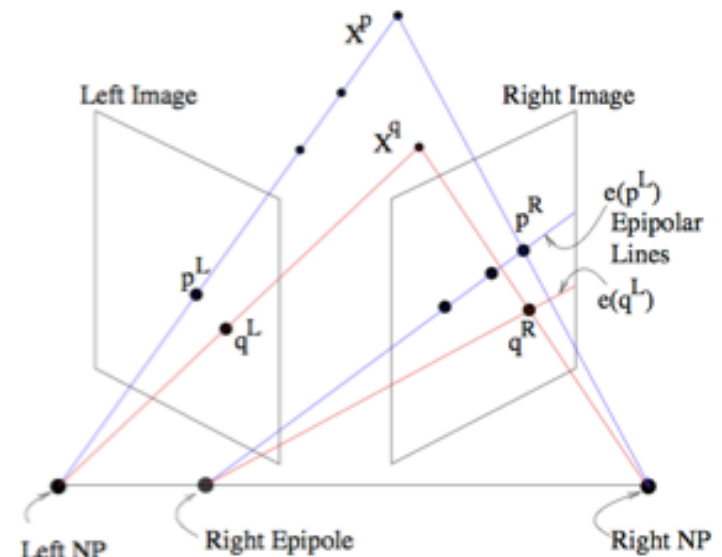
$\text{SVD}(A).V == \text{SVD}(A^TA).V == \underline{\text{SVD}(A^TA).U}$

## Points and Epipolar geometry: Essential Matrix

[http://www.cs.cmu.edu/~16385/s17/Slides/12.2\\_Essential\\_Matrix.pdf](http://www.cs.cmu.edu/~16385/s17/Slides/12.2_Essential_Matrix.pdf)



these three vectors are coplanar  $\mathbf{x}, \mathbf{t}, \mathbf{x}'$  so  
 $\mathbf{x}^\top (\mathbf{t} \times \mathbf{x}) = 0$  also  $(\mathbf{x} - \mathbf{t})^\top (\mathbf{t} \times \mathbf{x}) = 0$



<http://www.cs.toronto.edu/~jepson/csc420/notes/epiPolarGeom.pdf>

rigid motion	coplanarity
$\mathbf{x}' = \mathbf{R}(\mathbf{x} - \mathbf{t})$	$(\mathbf{x} - \mathbf{t})^\top (\mathbf{t} \times \mathbf{x}) = 0$
$(\mathbf{x}'^\top \mathbf{R})(\mathbf{t} \times \mathbf{x}) = 0$	
$(\mathbf{x}'^\top \mathbf{R})([\mathbf{t}_x] \mathbf{x}) = 0$	
$\mathbf{x}'^\top (\mathbf{R}[\mathbf{t}_x]) \mathbf{x} = 0$	
$\boxed{\mathbf{x}'^\top \mathbf{E} \mathbf{x} = 0}$	
Essential Matrix [Longuet-Higgins 1981]	

Longuet-Higgins equation	$\mathbf{x}'^\top \mathbf{E} \mathbf{x} = 0$
Epipolar lines	$\mathbf{x}^\top \mathbf{l} = 0$ $\mathbf{x}'^\top \mathbf{l}' = 0$ $\mathbf{l}' = \mathbf{E} \mathbf{x}$ $\mathbf{l} = \mathbf{E}^T \mathbf{x}'$
Epipoles	$\mathbf{e}'^\top \mathbf{E} = 0$ $\mathbf{E} \mathbf{e} = 0$ (points in normalized <u>camera</u> coordinates)

## Points and Epipolar geometry: Fundamental Matrix

[http://www.cs.cmu.edu/~16385/s17/Slides/12.3\\_Fundamental\\_Matrix.pdf](http://www.cs.cmu.edu/~16385/s17/Slides/12.3_Fundamental_Matrix.pdf)

$$\hat{\mathbf{x}}'^\top \mathbf{E} \hat{\mathbf{x}} = 0$$

The Essential matrix operates on image points expressed in  
**normalized coordinates**  
 (points have been aligned (normalized) to camera coordinates)

$$\hat{\mathbf{x}}' = \mathbf{K}^{-1} \mathbf{x}'$$

camera  
point

$$\hat{\mathbf{x}} = \mathbf{K}^{-1} \mathbf{x}$$

image  
point

Writing out the epipolar constraint in terms of image coordinates

$$\mathbf{x}'^\top \mathbf{K}'^{-\top} \mathbf{E} \mathbf{K}^{-1} \mathbf{x} = 0$$

$$\mathbf{x}'^\top (\mathbf{K}'^{-\top} [\mathbf{t}_x] \mathbf{R} \mathbf{K}^{-1}) \mathbf{x} = 0$$

$$\mathbf{x}'^\top \mathbf{F} \mathbf{x} = 0$$

## properties of the $\mathbf{E}$ matrix

Longuet-Higgins equation

$$\mathbf{x}'^\top \mathbf{E} \mathbf{x} = 0$$

Epipolar lines

$$\mathbf{x}^\top \mathbf{l} = 0$$

$$\mathbf{x}'^\top \mathbf{l}' = 0$$

$$\mathbf{l}' = \mathbf{E} \mathbf{x}$$

$$\mathbf{l} = \mathbf{E}^T \mathbf{x}'$$

Epipoles

$$\mathbf{e}'^\top \mathbf{E} = 0$$

$$\mathbf{E} \mathbf{e} = 0$$

(points in **image** coordinates)

## Points and Epipolar geometry: Fundamental Matrix

[http://www.cs.cmu.edu/~16385/s17/Slides/12.4\\_8Point\\_Algorithm.pdf](http://www.cs.cmu.edu/~16385/s17/Slides/12.4_8Point_Algorithm.pdf)

$$\begin{bmatrix} x'_m & y'_m & 1 \end{bmatrix} \begin{bmatrix} f_1 & f_2 & f_3 \\ f_4 & f_5 & f_6 \\ f_7 & f_8 & f_9 \end{bmatrix} \begin{bmatrix} x_m \\ y_m \\ 1 \end{bmatrix} = 0$$

Set up a homogeneous linear system with 9 unknowns

$$\begin{bmatrix} x_1x'_1 & x_1y'_1 & x_1 & y_1x'_1 & y_1y'_1 & y_1 & x'_1 & y'_1 & 1 \\ \vdots & \vdots \\ x_Mx'_M & x_My'_M & x_M & y_Mx'_M & y_My'_M & y_M & x'_M & y'_M & 1 \end{bmatrix} \begin{bmatrix} f_1 \\ f_2 \\ f_3 \\ f_4 \\ f_5 \\ f_6 \\ f_7 \\ f_8 \\ f_9 \end{bmatrix} = \mathbf{0}$$

**Torr & Murray, 1997, "The Development and Comparison of Robust Methods for Estimating the Fundamental Matrix"**

Consider the movement of a set of point image projections from an object which undergoes a rotation and non-zero translation between views. After the motion, the set of homogeneous image points  $\{\underline{x}_i\}$ ,  $i = 1, \dots, n$ , as viewed in the first image is transformed to the set  $\{\underline{x}'_i\}$  in the second image, positions related by

$$\underline{x}'^T \mathbf{F} \underline{x}_i = 0 \quad (1)$$

where  $\underline{x} = (x, y, \zeta)^T$  is a homogeneous image coordinate and

$$\mathbf{F} = \begin{bmatrix} f_1 & f_2 & f_3 \\ f_4 & f_5 & f_6 \\ f_7 & f_8 & f_9 \end{bmatrix}$$

is the fundamental Matrix (Faugeras 1992). Although  $3 \times 3$ , the matrix has only seven degrees of freedom because only the ratio of parameters is significant and because  $\det \mathbf{F} = 0$ . Throughout, underlining a symbol  $\underline{x}$  indicates the perfect or noise-free quantity, distinguishing it from  $x = \underline{x} + \Delta x$ , the value corrupted by noise (assumed Gaussian).

Faugeras 1992

In the case where at least eight point correspondences have been obtained between two images of an uncalibrated stereo rig, if we arbitrarily choose five of those correspondences and consider that they are the images of five points in general positions (i.e not four of them are coplanar), then it is possible to reconstruct the other three points and any other point arising from a correspondence between the two images in the projective coordinate system defined by the five points. This reconstruction is uniquely defined up to an unknown projective transformation of the environment.

In the case where at least eight point correspondences have been obtained between two images of an uncalibrated stereo rig, if we arbitrarily choose four of these correspondences and consider that they are the images of four points in general positions (i.e not coplanar), then it is possible to reconstruct the other four points and any other point arising from a correspondence between the two images in the affine coordinate system defined by the four points. This reconstruction is uniquely defined up to an unknown affine transformation of the environment.

from “Robust Parameter Estimation in Computer Vision”, 1999 Stewart

<https://citeseerx.ist.psu.edu/viewdoc/download?doi=10.1.1.7.3914&rep=rep1&type=pdf>

from “Computer Vision: Algorithms and Applications” by Szeliski

(Note, please consult author and book for any of this. use it's presented here for educational purposes only.)

see equations (1) and (2) of Zhang, Z. 1996, RR-2927, INRIA, ffinria-00073771

“Determining the Epipolar Geometry and its Uncertainty: A Review”.

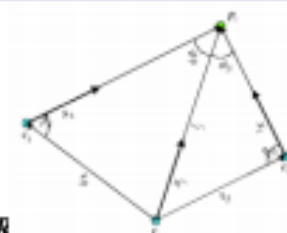
And:

<https://courses.cs.washington.edu/courses/csep576/11sp/pdf/SfM.pdf>

## Essential matrix

Co-planarity constraint:

$$\begin{aligned} \mathbf{x}' &\approx \mathbf{R}\mathbf{x} + \mathbf{t} \\ [\mathbf{t}]_{\times}\mathbf{x}' &\approx [\mathbf{t}]_{\times}\mathbf{R}\mathbf{x} \\ \mathbf{x}'^T[\mathbf{t}]_{\times}\mathbf{x}' &\approx \mathbf{x}'^T[\mathbf{t}]_{\times}\mathbf{R}\mathbf{x} \\ \mathbf{x}'^T\mathbf{E}\mathbf{x} &= 0 \text{ with } \mathbf{E} = [\mathbf{t}]_{\times}\mathbf{R} \end{aligned}$$



- Solve for  $\mathbf{E}$  using least squares (SVD)
- $\mathbf{t}$  is the least singular vector of  $\mathbf{E}$
- $\mathbf{R}$  obtained from the other two sing. vectors

## Fundamental matrix

Camera calibrations are unknown

$$\mathbf{x}'^T\mathbf{F}\mathbf{x} = 0 \text{ with } \mathbf{F} = [\mathbf{e}]_{\times}\mathbf{H} = \mathbf{K}'[\mathbf{t}]_{\times}\mathbf{R}\mathbf{K}^{-1}$$

- Solve for  $\mathbf{F}$  using least squares (SVD)
  - re-scale  $(\mathbf{x}_0, \mathbf{x}_1')$  so that  $|\mathbf{x}_i| \approx 1/2$  [Hartley]
- $\mathbf{e}$  (epipole) is still the least singular vector of  $\mathbf{F}$
- $\mathbf{H}$  obtained from the other two s.v.s
- “plane + parallax” (projective) reconstruction
- use self-calibration to determine  $\mathbf{K}$  [Pollefeys]

$\mathbf{F}$  has 7 degrees of freedom so can be estimated from at least 7 correspondence pairs.

For any point,  $\tilde{\mathbf{x}}'$ , in image 2,  $\mathbf{F}\tilde{\mathbf{x}}'$  defines a line in image 1 through which the point corresponding to  $\tilde{\mathbf{x}}'$  must pass. Similarly, for any point,  $\tilde{\mathbf{x}}$ , in image 1,  $\mathbf{F}^T\tilde{\mathbf{x}}$  defines a line in image 2 through which the point corresponding to  $\tilde{\mathbf{x}}$  must pass. All such lines, known as epipolar lines, pass through the epipoles, which are the null space of  $\mathbf{F}^T$  and  $\mathbf{F}$ , respectively.

## Points and Epipolar geometry: Fundamental Matrix

from Strang's "Introduction to Linear Algebra",

**Subspaces of matrix A which is mxn:**

row space:

is denoted  $C(A^T)$  and is a subspace of  $R^n$ .

all  $A^T y$ .

dimension is  $n \times r$ .

column space:

is denoted  $C(A)$  and is a subspace of  $R^m$ .

all  $A^* x$ . (the system  $A^* x = b$  is solvable iff  $b$  is in column space).

dimension is  $m \times r$ .

Null space:

denoted as  $N(A)$  and is a subspace of  $R^n$ . a.k.a. the kernel of  $A$ .

$Ax=0$ .

is orthogonal complement to ROW SPACE of  $A$ .

dimension is  $n \times (n-r)$ .

left null space:

denoted as  $N(A^T)$  and is a subspace of  $R^m$ . a.k.a. as the kernel of  $A^T$ .

all  $A^T y = 0$ . all column vectors  $x$  such that  $x^T A = 0^T$ .

is the orthogonal complement to COLUMN SPACE of  $A$ .

dimension is  $m \times (m-r)$ .

$Ax = \lambda x$ , where  $\lambda$  is an eigenvalue of  $A$ .

$\lambda$  tells whether the special vector  $x$  is stretched or shrunk or reversed or unchanged when it is multiplied by  $A$ .

nullspace entries: for eigenvalue lambda = 0 ,  $P^* x = 0^* x$

Singular matrices have  $\lambda = 0$  (and their determinants are 0).

$A^* f = 0$  (in terms of the subspaces of matrix  $A$ , we determine the null space by the  $A$ 's row space transposed times  $x = 0$  to find what's orthogonal to the rows)

$f$  orthogonal to  $A$  and eigenvalue=0 is smallest eigenvector of  $A$  which can be found with

$SVD(A).V$  or  $SVD(A^T A).V$  or  
 $SVD(A).U$  or  $SVD(A A^T).U$  then dimension reduction to rank=2 for  $F$  where  $A = U * S * V^T$

NOTE:

$SVD(A).U == SVD(A A^T).U == SVD(A A^T).V$

$SVD(A).V == SVD(A^T A).V == SVD(A^T A).U$

## Points and Epipolar geometry: Fundamental Matrix and **smallest eigenvalue**

from Wirtz and Guhr 2014,

“Distribution of the Smallest Eigenvalue in Complex and Real Correlated Wishart Ensembles”

<https://arxiv.org/pdf/1310.2467.pdf>

In linear discriminant analysis it [**smallest eigenvalue**] gives the leading contribution for the threshold estimate [21]. It is most sensitive to noise in the data [18]. In linear principal component analysis, ***the smallest eigenvalue determines the plane of closest fit [18]***. It is also crucial for the identification of single statistical outliers [17]. In numerical studies involving large random matrices, the condition number is used, which depends on the smallest eigenvalue [22, 23]. In wireless communication the Multi–Input–Multi– Output (MIMO) channel matrix of an antenna system is modeled by a random matrix [24]. The smallest eigenvalue of C yields an estimate for the error of a received signal [25, 26, 27]. In finance, the optimal portfolio is associated with the eigenvector to the smallest eigenvalue of the covariance matrix, which is directly related to the correlation matrix [28]. This incomplete list of examples shows the influence of the smallest eigenvalue in applications. ***Further information on the role of the smallest eigenvalue is given in Appendix A.***

[17] Barnett V, Lewis T. Outliers in Statistical Data. first edition ed. John Wiley & Sons; 1980.

[18] Gnanadesikan R. Methods for Statistical Data Analysis of Multivariate Observations. Second edition ed. John Wiley & Sons; 1997.

Torr & Murray, 1997, "The Development and Comparison of Robust Methods for Estimating the Fundamental Matrix"

[https://www.robots.ox.ac.uk/ActiveVision/Publications/torr\\_murray\\_ijcv1997/torr\\_murray\\_ijcv1997.pdf](https://www.robots.ox.ac.uk/ActiveVision/Publications/torr_murray_ijcv1997/torr_murray_ijcv1997.pdf)

2.2. *Orthogonal Least Squares Regression: Method OR*

Ignoring for the moment the problem of enforcing the rank 2 constraint, given  $n \geq 8$  correspondences this system appears an archetype for solution by linear least squares regression. Linear here refers to linearity in the parameters  $f_i$  — equation (1) written out is just

$$\begin{aligned} f_1 \underline{x}_i' \underline{x}_i + f_2 \underline{x}_i' \underline{y}_i + f_3 \underline{x}_i' \zeta + f_4 \underline{y}_i' \underline{x}_i + \\ f_5 \underline{y}_i' \underline{y}_i + f_6 \underline{y}_i' \zeta + f_7 \underline{x}_i \zeta + f_8 \underline{y}_i \zeta + f_9 \zeta^2 = 0 . \end{aligned}$$

Because errors exist in all the measured coordinates  $x, y, x', y'$ , orthogonal least squares (Pearson 1901) rather than ordinary least squares should be used, minimizing the sum of the squares of the distances shown in part (a) rather than (b) of Figure 2.

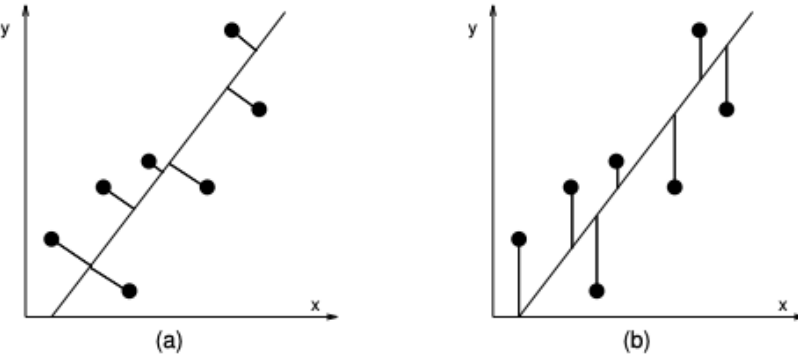


Fig. 2. The (a) orthogonal and (b) ordinary least squares distances.

Consider fitting a hyperplane  $\mathbf{f} = (f_1, f_2, \dots, f_p)$  through a set of  $n$  points in  $\mathcal{R}^p$  with coordinates  $\mathbf{z}_i = (z_{i1}, z_{i2}, \dots, z_{ip})$ , taking the centroid of the data as origin. (Centring is a standard statistical technique that involves shifting the coordinate system of the data points so that the centroid lies at the origin. The best fitting hyperplane passes through the centroid of the data (Pearson 1901).) Assuming that the noise is Gaussian and that the elements of  $\mathbf{z}$  have equal variance<sup>1</sup>, the hyperplane  $\mathbf{f}$  with maximum likelihood is estimated by minimizing the perpendicular sum of Euclidean distances from the points to the plane (Pearson 1901; Kendall & Stuart 1983)

$$\min_{\mathbf{f}} \sum_{i=1}^n (\mathbf{f}^\top \mathbf{z}_i)^2$$

**Method S1.**

The orthogonal least squares method (OR) will in fact produce a sub-optimal estimate of  $F$  because the residuals in the minimization

$$\begin{aligned} r_i = f_1 \underline{x}_i' \underline{x}_i + f_2 \underline{x}_i' \underline{y}_i + f_3 \underline{x}_i' \zeta + f_4 \underline{y}_i' \underline{x}_i + \\ + f_5 \underline{y}_i' \underline{y}_i + f_6 \underline{y}_i' \zeta + f_7 \underline{x}_i \zeta + f_8 \underline{y}_i \zeta + f_9 \zeta^2 \quad (2) \end{aligned}$$

are not Gaussianly distributed. The cause of this is

## Torr & Murray, 1997, "The Development and Comparison of Robust Methods for Estimating the Fundamental Matrix"

[https://www.robots.ox.ac.uk/ActiveVision/Publications/torr\\_murray\\_ijcv1997/torr\\_murray\\_ijcv1997.pdf](https://www.robots.ox.ac.uk/ActiveVision/Publications/torr_murray_ijcv1997/torr_murray_ijcv1997.pdf)

### Method S2. Luong and Faugeras (1993)

the epipolar line  $\mathbf{F}'\mathbf{x}$  in image two. Noisy measurements will however not lie on their associated epipolar lines exactly. The perpendicular distance of a point  $\mathbf{x}$  to the predicted epipolar line  $\mathbf{x}'^\top \mathbf{F}$  in the first image is

$$e_1 = \frac{xr_x + yr_y + r_\zeta}{(r_x^2 + r_y^2)^{1/2}} = \frac{r}{(r_x^2 + r_y^2)^{1/2}}.$$

and the distance of a point  $\mathbf{x}'$  to the epipolar line  $\mathbf{F}\mathbf{x}$  in the second image is

$$e_2 = \frac{r}{(r_{x'}^2 + r_{y'}^2)^{1/2}}.$$

its epipolar line is used. This ensures that each image receives equal consideration. The distance  $e = (e_1^2 + e_2^2)^{1/2}$  is referred to as the epipolar distance. It is assumed that the errors in the measured location of each point are Gaussian with variance  $\sigma^2$ . If the co-

$w_E$ , so that  $e = rw_E$ . Effectively then the epipolar weighting is

$$w_E = \left( \frac{1}{r_x^2 + r_y^2} + \frac{1}{r_{x'}^2 + r_{y'}^2} \right)^{1/2},$$

which is not dissimilar to the Sampson weighting

$$w_S = \left( \frac{1}{r_x^2 + r_y^2 + r_{x'}^2 + r_{y'}^2} \right)^{1/2}.$$

In summary, three least squares methods with different error terms have been discussed:

1. Method OR uses the sum of squares of *algebraic distances*:

$$R^2 = \sum r_i^2, \text{ where } r_i = \mathbf{x}_i'^\top \mathbf{F} \mathbf{x}_i.$$

2. Method S1 uses the sum of squares of the Sampson distances:

$$D^2 = \sum (w_{Si} r_i)^2 = \sum (r_i / \nabla r_i)^2 = \sum d_i^2.$$

3. Method S2 uses the sum of squares of the epipolar distances:

$$E^2 = \sum (w_{Ei} r_i)^2 = \sum (e_{1i}^2 + e_{2i}^2) = \sum e_i^2.$$

In terms of probability distributions, the first corresponds to something intractable, the second is a first order approximation to a  $\chi^2$  distribution, and the third is a  $\chi^2$  distribution.

## Statistics of matching correspondence

from “Robust Parameter Estimation in Computer Vision”, 1999 Stewart

<https://citeseerx.ist.psu.edu/viewdoc/download?doi=10.1.1.7.3914&rep=rep1&type=pdf>

### **Robust Estimation**

**breakdown point:** the minimum fraction of outlying data that can cause an estimate to diverge arbitrarily far from the true estimate. (e.g. for least squares, 1 outlier can harm the estimate, so the breakdown point is 0). a breakdown point of 0.5 is traditionally used.

**influence function:** the change in an estimate caused by insertion of outlying data as a function of the distance of the data from the (uncorrupted) estimate. (e.g. for least squares, the influence function is simply proportional to the distance of the point from the estimate.) influence function should approach 0 with increasing distance.

**statistical efficiency:** ratio of minimum possible variance to the actual variance of an estimate. the minimum possible variance is determined by a distribution such as a gaussian. the upper bound of efficiency is then 1.

Linear Regression or estimation of univariate or multivariate location and scatter are used.

Let  $\mathbf{X} = \{\mathbf{x}_i\}$  be a set of data points (vectors)

Let  $\mathbf{a}$  be a k-dimensional parameter vector to be estimated.

$r_i(\mathbf{x}_i, \mathbf{a}) = r(\mathbf{x}_i, \mathbf{a})$  is the objective function is defined in terms of an error distance or residual function, a true geometric distance is ideal. euclidean, mahalanobis of the covariance matrix, etc.

(Mahalanobis distance is a measure of the distance between a point and a distribution in terms of standard deviations.)

### **M-estimators and least-median of squares**

## Statistics of matching correspondence

from “Robust Parameter Estimation in Computer Vision”, 1999 Stewart

<https://citeseerx.ist.psu.edu/viewdoc/download?doi=10.1.1.7.3914&rep=rep1&type=pdf>

**M-estimators:** generalizations of maximum likelihood and least squares.

$\sigma_i^2$  = variance (scale) assoc. w/ scalar  $r_{i,a}$

$\rho(u)$  = a robust loss function

$\hat{\mathbf{a}}$  is the M-estimator of  $\mathbf{a}$ .

$$\hat{\mathbf{a}} = \operatorname{argmin}_{\mathbf{a}} \sum_{\mathbf{x}_i \in X} \rho(r_{i,\mathbf{a}} / \sigma_i)$$

$\psi(u) = \rho'(u)$  is essentially proportional to the influence function.

$w(u) \cdot u = \psi(u)$  is a weight function.

iteratively re-weighted least-squares (IRLS) alternates between calculating weights

$w_i = w(r_{i,a}/\sigma_i)$  using the current estimate of  $\mathbf{a}$  then solving following eqn. to estimate

$\mathbf{a}$  with fixed weights.

$$\sum_{\mathbf{x}_i \in X} \psi(r_{i,\mathbf{a}} / \sigma_i) \frac{dr_{i,\mathbf{a}}}{d\mathbf{a}} \frac{1}{\sigma_i} = 0.$$

Beaton and Tukey [4]	$\rho(u) = \begin{cases} \frac{a^2}{6} [1 - (1 - (\frac{u}{a})^2)^3] &  u  \leq a \\ \frac{a^2}{6} &  u  > a \end{cases}$	$\psi(u) = \begin{cases} u [1 - (\frac{u}{a})^2]^2 &  u  \leq a \\ 0 &  u  > a \end{cases}$
Cauchy [32]	$\rho(u) = \frac{b^2}{2} \log[1 + (\frac{u}{b})^2]$	$\psi(u) = \frac{u}{1+(u/b)^2}$
Huber [34, Chapter 7]	$\rho(u) = \begin{cases} \frac{1}{2}u^2 &  u  \leq c \\ \frac{1}{2}c(2 u  - c) & c <  u  \end{cases}$	$\psi(u) = \begin{cases} 1 &  u  \leq c \\ c \frac{u}{ u } &  u  > c \end{cases}$

Table 1: Three different robust loss functions,  $\rho(u)$ , and associated  $\psi$  functions. The “tuning parameters”  $a$ ,  $b$  and  $c$  are often tuned to obtain 95% efficiency [32].

## Statistics of matching correspondence

from “Robust Parameter Estimation in Computer Vision”, 1999 Stewart

<https://citeseerx.ist.psu.edu/viewdoc/download?doi=10.1.1.7.3914&rep=rep1&type=pdf>

**Least-Median of Squares:** has a breakdown point of 0.5.

$$\hat{\mathbf{a}} \text{ is the LMS estimate of } \mathbf{a}. \quad \hat{\mathbf{a}} = \underset{\mathbf{a}}{\operatorname{argmin}} \underset{\mathbf{x}_i \in X}{\operatorname{median}} r_{i,\mathbf{a}}^2.$$

because the median is not differentiable, search techniques are needed.

e.g. for regression lines, can computationally solve for median exactly and efficiently.

a random sampling technique: randomly select a number of  $k$ -point subsets of the  $N$  data points. A parameter vector,  $\mathbf{a}_s$ , is fit to the points in each subset,  $s$ . Each  $\mathbf{a}_s$  is tested as a hypothesized fit by calculating the squared residual distance  $(r_{ias})^2$  of each of the  $N-k$  points in  $X-s$  and finding the median. The  $\mathbf{a}_s$  corresponding to the smallest median over  $S$  subsets is chosen as the estimate,  $\hat{\mathbf{a}}$ . Overall, this computation requires  $O(S N)$  time using linear-time median finding techniques.

Determining the number of subsets  $S$  is important.  $S$  needs to be large enough to have high probability of containing all “good” points, that is, no outliers.

$p$  is the minimum fraction of good points.

$p^k$  is the probability that a set contains all good points.

$$P_g = 1 - (1 - p^k)^S.$$

choose  $P_g$  and solve for  $S$ :

$P_g$	$k$	$p$	$S$
0.99	3	0.5	35
0.99	6	0.6	97
0.99	6	0.5	293

## Statistics of matching correspondence

from “Robust Parameter Estimation in Computer Vision”, 1999 Stewart

<https://citeseerx.ist.psu.edu/viewdoc/download?doi=10.1.1.7.3914&rep=rep1&type=pdf>

### Least-Median of Squares (cont.):

$\hat{\mathbf{a}}$  can be used to refine the fit.

$s^*$  is the subset used to form  $\hat{\mathbf{a}}$ .

$\Phi^{-1}$  is the inverse of the cumulative normal distribution.

$$\hat{\sigma} = 1/\Phi^{-1}(0.75) \left(1 + \frac{5}{N - k}\right) \sqrt{\underset{\mathbf{x}_i \in X - s^*}{\text{median}} r_{i,\hat{\mathbf{a}}}^2},$$

if all N points are sampled from a normal distribution with variance  $\sigma^2$ , then  $\sigma^\wedge \rightarrow \sigma$  as  $N \rightarrow \infty$ .  
can choose data points such that  $(r_{ias})^2 < (\theta \sigma^\wedge)^2$  where  $\theta$  is constant, typically about 2.5 then re-estimate  $\hat{\mathbf{a}}$ .

### Random Sample Consensus (RANSAC):

a minimal subset random sampling search technique, the objective function to be maximized is the number of data points (inliers) having absolute residuals smaller than a predefined value.

Equivalently, this may be viewed as minimizing the number of outliers, which may then be viewed as a binary robust loss function that is 0 for small (absolute) residuals, 1 for large absolute residuals, and has a discontinuous transition at  $\theta$ .

**Torr & Murray, 1997, "The Development and Comparison of Robust Methods for Estimating the Fundamental Matrix"**

[https://www.robots.ox.ac.uk/ActiveVision/Publications/torr\\_murray\\_ijcv1997/torr\\_murray\\_ijcv1997.pdf](https://www.robots.ox.ac.uk/ActiveVision/Publications/torr_murray_ijcv1997/torr_murray_ijcv1997.pdf)

**Using RANSAC w/ 8-point or 7-point methods:**

RANSAC uses iterations over random subsets of size 7 or 8 of the total point set (which is usually over-determined, having more than 8 points), solves for the fundamental matrix ( $F$ ), evaluates the fit using epipolar projections of all points, and keeps the best  $F$ .

The number of iterations is pre-calculated for the probability that all points are not outliers. Then upon each improved  $F$  in the iterations, the number of iterations is readjusted downwards.

*Table 3.* The number  $m$  of subsamples required to ensure  $\Upsilon \geq 0.95$  for given  $p$  and  $\epsilon$ , where  $\Upsilon$  is the probability that all the data points selected in one subsample are non-outliers.

Features $p$	Fraction of Contaminated Data, $\epsilon$						
	5%	10%	20%	25%	30%	40%	50%
2	2	2	3	4	5	7	11
3	2	3	5	6	8	13	23
4	2	3	6	8	11	22	47
5	3	4	8	12	17	38	95
6	3	4	10	16	24	63	191
7	3	5	13	21	35	106	382
8	3	6	17	29	51	177	766

## Fundamental Matrix: 7 point algorithm

(see src/.../EpipolarTransformer.java)

(see [https://www.robots.ox.ac.uk/~vgg/hzbook/code/vgg\\_multiview/vgg\\_F\\_from\\_7pts\\_2img.m](https://www.robots.ox.ac.uk/~vgg/hzbook/code/vgg_multiview/vgg_F_from_7pts_2img.m) from "Multiple View Geometry in Computer Vision  
Second Edition, by Hartley and Zisserman)

### **7-Point algorithm** (for use with uncalibrated cameras):

(1) Transform the coordinates

(2) build matrix A with the normalized x,y points

(3) compute linear least square solution to the least eigenvector of f.

    solve  $A = U * D * V^T$  for  $A*f = [..x....]*f = 0$

    A has rank 7. **f has rank 2.** calculate [U,D,V] from svd(A)

(4)  $[U,D,V] = \text{svd}(F,0);$

    The homogeneous system  $AX = 0$  : X is the null space of matrix A.

    The system is nullable because rank 7 < number of columns, 9.

    The nullable system must have a solution other than trivial where  $|A| = 0$ .

    There should be  $9-7=2$  linearly independent vectors  $u_1, u_2, \dots, u_{n-r}$  that span the null space of A.

    The right null space of A reduced by SVD is then 2D and the last

    2 columns of V can be extracted and reshaped to [3x3] as F1 and F2.

    A linear convex combination of F1 and F2 form the estimate of F.

$F = \alpha*F1 + (1 - \alpha)*F2$  where  $\alpha$  is between 0 and 1

    The eigenvalues of F are possible only if the determinant of F is 0.

$\det A = 0 \implies \det(\alpha*F1 + (1 - \alpha)*F2) = 0$

    because  $\det(F1 + F2) \neq \det(F1) + \det(F2)$ , have to step through the

    determinant of the sums, and group the terms by  $a^3, a^2, a^1$ , and  $a^0$   
    and then solve for the cubic roots as the values of 'a'.

    The determinant of F is a polynomial function, the characteristic

    polynomial whose degree is the order of the matrix, which is 3 in this  
    case. Therefore, the answer(s) to  $\det(F) = 0$  requires the cubic  
    roots of the equation.

    After the cubic root(s) are solved, they are back substituted into :

$F_i = a(i) * FF\{1\} + (1-a(i)) * FF\{2\};$

        to get the solutions  $F_i$  which may be one or 3 solutions

(5) denormalize the fundamental matrix

    The related part of the normalization equation:  $\text{inv}(T_2) * F * \text{inv}(T_1)$

    so denormalizing is:

$F = (T_1)^T * F * T_2$

(6) validate the 1 to 3 solutions:

(7) estimate the error in the fundamental matrix by calculating epipolar  
    lines for points in image 1 and find their nearest points in image 2  
    and measure the perpendicular distance from the epipolar line for  
    those nearest points.

Torr, Zisserman, & Maybank 1996, “Robust Detection of Degenerate Configurations whilst Estimating the Fundamental Matrix <https://www.robots.ox.ac.uk/~phst/Papers/CVIU97/m.ps.gz>

## 2 Degeneracy and the Fundamental matrix

Suppose that a camera takes two noise free images of a 3D object, and undergoes a rotation and non-zero translation between the two images. The set of image points  $\{\underline{x}_i\}, i = 1, \dots, n$ , in the first image (we adopt the convention of signifying noise free data by underlining it) is transformed to the set  $\{\underline{x}'_i\}$ , in the second, where  $\underline{x}_i$  and  $\underline{x}'_i$  have homogeneous coordinates,  $\underline{x}_i = (\underline{x}_i, \underline{y}_i, 1)^\top$ , and  $\underline{x}'_i = (\underline{x}'_i, \underline{y}'_i, 1)^\top$ . The two sets of image points are related by

$$\underline{x}'_i^\top \mathbf{F} \underline{x}_i = 0 \quad 1 \leq i \leq n \tag{1}$$

where  $\mathbf{F}$  is a  $3 \times 3$  matrix of rank 2. It is known as the fundamental matrix [11, 18].

Recall that data are degenerate if the true data (the noise free correspondences) admit multiple solutions for the fundamental matrix. It can be seen that an understanding is required of cases that lead to the true data being degenerate. The next subsection analyses all such cases.

### 2.1 Geometric Degeneracy

A perfect (i.e. noise free and no outliers) set of correspondences:  $\{\underline{x}_i\} \leftrightarrow \{\underline{x}'_i\}, i = 1, \dots, n$ , is geometrically degenerate with respect to  $\mathbf{F}$  if it fails to define a unique epipolar transform, or equivalently if there exist linearly independent rank two matrices,  $\mathbf{F}_j, j = 1, 2$ , such that

$$\underline{x}'_i^\top \mathbf{F}_1 \underline{x}_i = \underline{x}'_i^\top \mathbf{F}_2 \underline{x}_i = 0 \quad (1 \leq i \leq n) . \tag{2}$$

## Points and Epipolar geometry: Fundamental Matrix: ambiguous solutions

Torr, Zisserman, & Maybank 1996, “Robust Detection of Degenerate Configurations whilst Estimating the Fundamental Matrix <https://www.robots.ox.ac.uk/~phst/Papers/CVIU97/m.ps.gz>

for n correspondences >= 8 in general position: dim(N) = 1 : There is no degeneracy:

for n correspondences == 7 or for both camera optical centers and and any number of 3D points lie on a quadric surface referred to as the critical

dim(N) = 2 imposing the constraint that FM rank=2, one must solve the cubic equation in alpha, and that has 1 or 3 solutions. if it has 1 solution, it is not degenerate.

dim(N) = 3 this structure can arise from an observation of a special type of structure (a plane) or from the camera undergoing a special type of motion (a rotation about its optic center)

dim(N) = 4 points are not in general position, but lie on a line

Torr, Zisserman, & Maybank 1996, “Robust Detection of Degenerate Configurations whilst Estimating the Fundamental Matrix <https://www.robots.ox.ac.uk/~phst/Papers/CVIU97/m.ps.gz>

1. Varieties  $V$  of dimension 3.

- (a) *Fundamental matrix*, degree 2, DOF 7, correspondences 7, for 1 or 3 solutions, 8 for unique solution.

$$\mathbf{x}'^\top \mathbf{F} \mathbf{x} = 0 \quad \text{where} \quad \mathbf{F} = \begin{bmatrix} f_1 & f_2 & f_3 \\ f_4 & f_5 & f_6 \\ f_7 & f_8 & f_9 \end{bmatrix} \quad (10)$$

- (b) *Affine fundamental matrix*, degree 1, DOF 4, correspondences 4.

$$\mathbf{x}'^\top \mathbf{F}_A \mathbf{x} = 0 \quad \text{where} \quad \mathbf{F}_A = \begin{bmatrix} 0 & 0 & a_1 \\ 0 & 0 & a_2 \\ a_3 & a_4 & a_5 \end{bmatrix}. \quad (11)$$

- (c) *Translation fundamental matrix*, degree 2, DOF 2, correspondences 2.

$$\mathbf{x}'^\top \mathbf{F}_T \mathbf{x} = 0 \quad \text{where} \quad \mathbf{F}_T = \begin{bmatrix} 0 & g_3 & -g_2 \\ -g_3 & 0 & g_1 \\ g_2 & -g_1 & 0 \end{bmatrix}. \quad (12)$$

**Torr, Zisserman, & Maybank 1996, “Robust Detection of Degenerate Configurations whilst Estimating the Fundamental Matrix** <https://www.robots.ox.ac.uk/~phst/Papers/CVIU97/m.ps.gz>

2. Varieties  $V$  of dimension 2.

- (a) *Quadratic image transformation*,  $\mathbf{Q}$ , degree 4, DOF 14, correspondences 7;

$$\mathbf{x}' = \mathbf{F}_1 \mathbf{x} \times \mathbf{F}_2 \mathbf{x}, \text{ where } \mathbf{F}_1, \mathbf{F}_2 \text{ are } 3 \times 3 \text{ fundamental matrices.}$$

- (b) *Projective image transformation*, degree 4, DOF 8, correspondences 4.

$$\mathbf{x}' = \mathbf{H} \mathbf{x} \quad \text{where} \quad \mathbf{H} = \begin{bmatrix} h_1 & h_2 & h_3 \\ h_4 & h_5 & h_6 \\ h_7 & h_8 & h_9 \end{bmatrix}. \quad (13)$$

- (c) *Affine image transformation*, degree 1, DOF 6, correspondences 3.

$$\mathbf{x}' = \mathbf{K} \mathbf{x} \quad \text{where} \quad \mathbf{K} = \begin{bmatrix} k_1 & k_2 & k_3 \\ k_4 & k_5 & k_6 \\ 0 & 0 & 1 \end{bmatrix}. \quad (14)$$

- (d) *Image translation*, degree 1, DOF 1, correspondence 1.

$$\mathbf{x}' = \mathbf{L} \mathbf{x} \quad \text{where} \quad \mathbf{L} = \begin{bmatrix} 1 & 0 & t_x \\ 0 & 1 & t_y \\ 0 & 0 & 1 \end{bmatrix}. \quad (15)$$

- (e) *No Motion*, degree 1, DOF 0, correspondences 0.

Table 1: Models that are fitted to sets of correspondences. The models (top to bottom) are given in order of decreasing generality. For example the affine fundamental matrix and the translational fundamental matrix are both special cases of the fundamental matrix.

## Points and Epipolar geometry:Fundamental Matrix: ambiguous geometries

**Torr, Zisserman, & Maybank 1996, “Robust Detection of Degenerate Configurations whilst Estimating the Fundamental Matrix** <https://www.robots.ox.ac.uk/~phst/Papers/CVIU97/m.ps.gz>

### 7.3 Using RANSAC to Detect Degeneracy—PLUNDER-DL

number of dependent significance levels. Rather what is required is some sort of score function for each of the fitted models; and this score function must perform be composed of some combination of the available information: the number of inliers and outliers, and the degree and dimensionality of the model. The choice of scoring function must be dictated by the application of the algorithm. In order to accomplish this within this paper we have adapted the ideas of Minimum Message Length (MML) [14] and Minimum Description Length (MDL) [38]. The general idea of these methods is to minimize the binary digits (*bits*) needed to encode a signal in order to send the signal over a communication channel and decode it on the other side of the channel. The idea that

The new PLUNDER-DL approach differs from MDL in that it does not assume knowledge of the residuals or their probability distributions, as it encodes only the deterministic and not the stochastic part of the signal (which is assumed to be small). All that is needed is the set of inliers and the set of outliers to the model. In the results section we will argue that in the vast majority of cases further sophistry is unnecessary and adds an extra computational burden for little gain.

Consider a point in  $\mathcal{R}^4$ , in order to encode this point 4 coordinates are needed. Let the image size be  $R \times R$  window, e.g.  $512 \times 512$ , and the coordinates are measured up to a resolution of  $\epsilon$ , e.g. the Harris corner detector [15, 17] can achieve sub-pixel accuracy of 0.1 pixels in the location of a point. If a point is located within  $\mathcal{R}^4$  then the minimum encoding length for each coordinate is  $\log \frac{R}{\epsilon}$ . Let the model parameters storage be  $\log b$ . As a fundamental matrix has 7 DOF then it may be encoded by seven parameters. As the variety defined by  $\mathbf{F}$  has dimension three, each inlier may be encoded by 3 coordinates. Outliers to the fundamental matrix may not be so economically described being points in  $\mathcal{R}^4$ , and hence require 4 coordinates to describe them. Thus if the fit to the fundamental matrix provides  $n_i^F$  inliers and  $n_o^F$  outliers the PLUNDER-DL code length is

$$\mathbf{PL}(\mathbf{F}) = (3n_i^F + 4n_o^F) \log a + 7 \log b . \quad (30)$$

If for a homography there are  $n_i^H$  inliers and  $n_o^H$  outliers then the corresponding PLUNDER-DL score is (recalling that the dimension of  $\mathbf{H}$  is 2 and there are 8 degrees of freedom)

$$\mathbf{PL}(\mathbf{H}) = (2n_i^H + 4n_o^H) \log a + 8 \log b . \quad (31)$$

1. Estimate the set of inliers for each model using RANSAC, as described in Section 6.
2. Compute PLUNDER-DL scores for each model using (33).
3. Accept the model with the lowest PLUNDER-DL score.

Table 5: A brief summary of PLUNDER-DL.

excepting, that a threshold  
is used for calculating inliers

In the absence of *a priori* information we choose to store the parameters with the same amount of storage as the data, i.e.  $\log b = \log a$ .

$$\mathbf{PL} = (n_i \text{ dimension of model} + 4n_o) + \text{DOF} , \quad (33)$$

**Torr, Zisserman, & Maybank 1996, “Robust Detection of Degenerate Configurations whilst Estimating the Fundamental Matrix** <https://www.robots.ox.ac.uk/~phst/Papers/CVIU97/m.ps.gz>

#### 4.1 Determining Goodness of Fit

Within this section the traditional  $\chi^2$  method of determining the goodness of fit is outlined, and its deficiencies revealed. Assuming that the image coordinates are perturbed by Gaussian noise with mean zero and known variance  $\sigma^2$  (thus there are no outliers), then the distance of a perturbed point correspondence from the algebraic variety defined by the fundamental matrix also follows a Gaussian distribution. Hence the sum of squares of these distances follows a  $\chi^2$  distribution. The acceptability of a given  $\mathbf{F}$  may be judged in terms of its errors. The true fundamental matrix is unknown and an estimate must performe be used in its place. If the estimate is sufficiently close to the true fundamental matrix then the sum of squares of distances to the estimate  $d_V$ , divided by their standard deviation, has a  $\chi^2$  distribution with  $d_f = n - 7$  degrees of freedom, where  $n$  is the number of image correspondences, and seven is the number of degrees of freedom of the fundamental matrix. The suitability of a given  $\mathbf{F}$  may be tested under the assumption that a fit is good if it lies within the *critical region* of all solutions, defined as those with sum of squares of distances below  $T_F = \chi_{d_f}^2(\alpha)$ , where  $\alpha$  is the required degree of confidence, i.e. the critical region in the space of  $\mathbf{F}$  is given by

$$\{\mathbf{F} | D_V(\mathbf{F}) \leq T_F\} \quad (21)$$

typically  $\alpha = 95\%$ . We have given two other types of fundamental matrix that might occur in practice, the error  $D_V(\mathbf{F}_T)$  has  $d_f = n - 2$  degrees of freedom,  $D_V(\mathbf{F}_A)$  has  $d_f = n - 4$  degrees of freedom.

## Points and Epipolar geometry: Fundamental Matrix: ambiguous solutions

**Torr, Zisserman, & Maybank 1996, “Robust Detection of Degenerate Configurations whilst Estimating the Fundamental Matrix** <https://www.robots.ox.ac.uk/~phst/Papers/CVIU97/m.ps.gz>

Model	corr	Figure 3	Figure 5	Figure 6	Figure 7	Figure 8	Figure 9
Number of matches $n$		36	142	406	190	80	332
Fundamental	7	<u>31/120</u>	134/471	305/1326	131/645	<u>75/252</u>	241/1094
Translation	2	27/119	88/482	305/1322	69/693	14/308	241/1089
Affine Fundamental	4	28/120	128/444	304/1324	64/700	46/278	240/1092
Quadratic	18	31/100	131/324	270/1102	<u>127/524</u>	38/262	240/866
Projectivity	8	27/98	127/318	<u>268/1096</u>	71/626	36/256	239/858
Affinity	6	<u>27/96</u>	<u>128/315</u>	239/1152	53/600	32/262	<u>239/856</u>

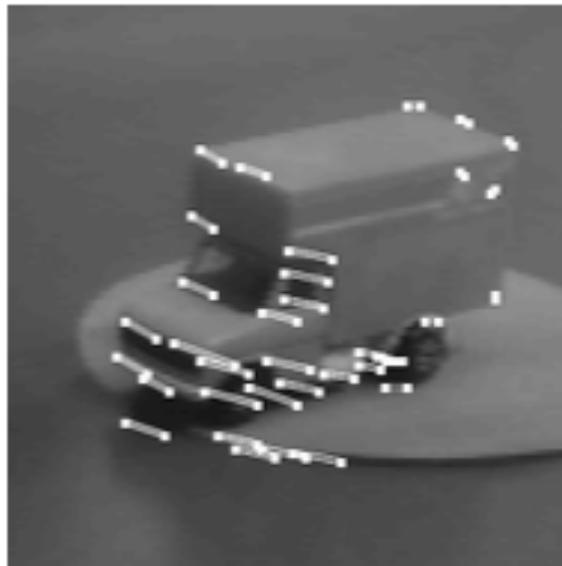
Table 6: For each model the number of inliers/PLUNDER-DL score ( $n_i/\text{PL}$ ) is given. The model selected is underlined. corr refers to the minimum number of correspondences needed to instantiate a model.

## Points and Epipolar geometry: Fundamental Matrix: ambiguous solutions

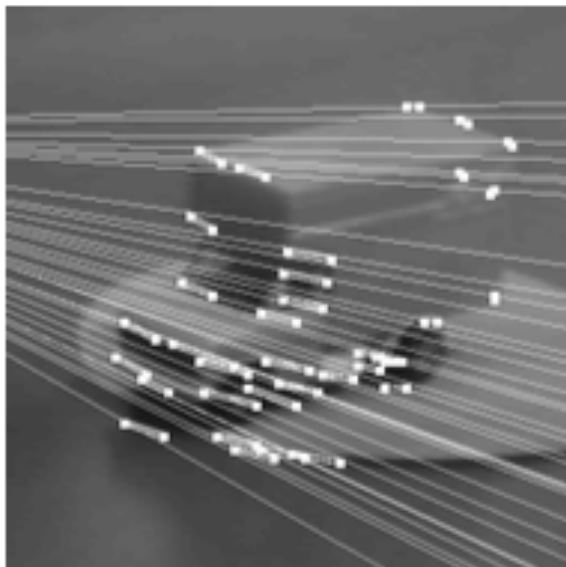
**Torr, Zisserman, & Maybank 1996, “Robust Detection of Degenerate Configurations whilst Estimating the Fundamental Matrix** <https://www.robots.ox.ac.uk/~phst/Papers/CVIU97/m.ps.gz>



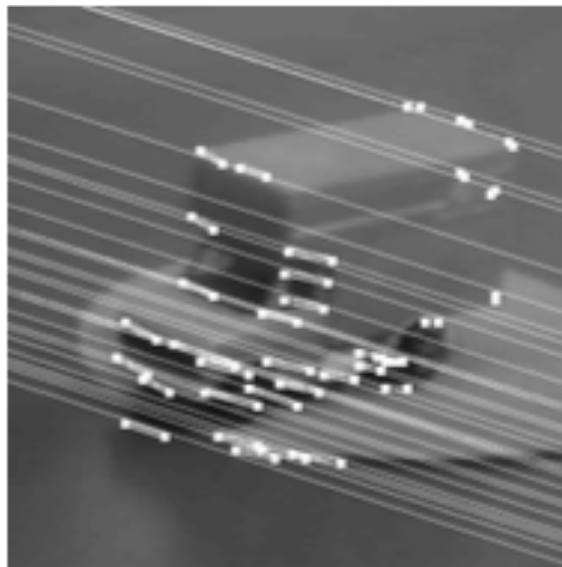
(a)



(b)



(c)



(d)

Figure 3: Rotating toy truck sequence (a) first image (b) second image with correspondences from (a) to (b) superimposed, (c) (d) Two epipolar geometries that fit the correspondences shown in Figure 3 (b) equally well. It can be seen that the data are degenerate. (d) is an affine camera epipolar geometry with parallel epipolar lines.

The model selected is an affinity, established by 3 point correspondences; 27 points are consistent with the affinity and 31 with a full fundamental matrix which has  $7 - 3 = 4$  more degrees of freedom. The data are thus clearly degenerate with respect to  $F$ , with most of the points lying on the plane of the truck.

Torr, Zisserman, & Maybank 1996, “Robust Detection of Degenerate Configurations whilst Estimating the Fundamental Matrix <https://www.robots.ox.ac.uk/~phst/Papers/CVIU97/m.ps.gz>



(a)



(b)

Figure 5: (a) First image and (b) second image with matches. The camera motion is composed of a large rotation of the camera about the optic axis and translation along the line of sight.

In Figure 5 the camera motion combines a translation perpendicular to the image plane with a cyclotorsion. The best fitting degenerate model is an affinity with 128 points, as expected.

Torr, Zisserman, & Maybank 1996, “Robust Detection of Degenerate Configurations whilst Estimating the Fundamental Matrix <https://www.robots.ox.ac.uk/~phst/Papers/CVIU97/m.ps.gz>



(a)



(b)



(c)



(d)

Figure 6: Two images from the gun fighter sequence. The camera

is tracking to the right and the gun fighter raises his gun. (a) first image, (b) second image and matches, (c) inliers, and (d) outliers.

Figure 6 (a)(b) shows a mobile gun fighter viewed by a tracking camera. The gunfighter is moving to the right as the camera moves in parallel to keep him in the center of the image. Points in independent motion on the gun fighter are identified if they are inconsistent with the motion model chosen for the background motion. The data support a projectivity as most of the correspondences are on the saloon wall.

## Points and Epipolar geometry: Fundamental Matrix: ambiguous solutions

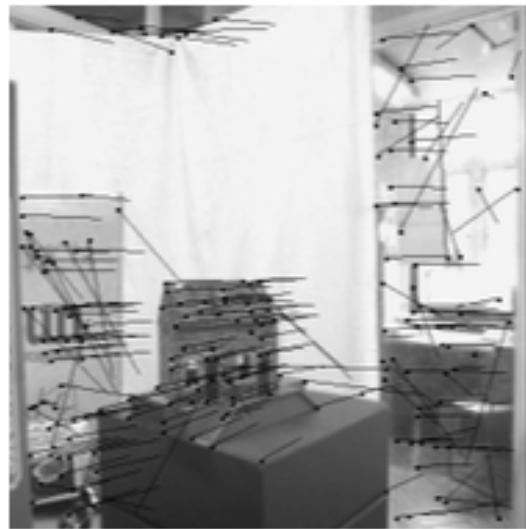
**Torr, Zisserman, & Maybank 1996, “Robust Detection of Degenerate Configurations whilst Estimating the Fundamental Matrix** <https://www.robots.ox.ac.uk/~phst/Papers/CVIU97/m.ps.gz>



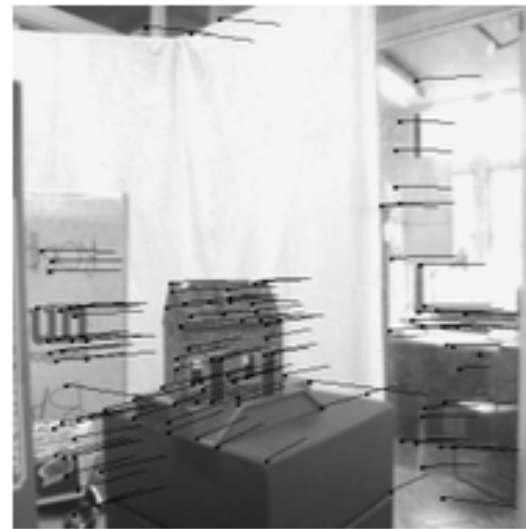
(a)



(b)



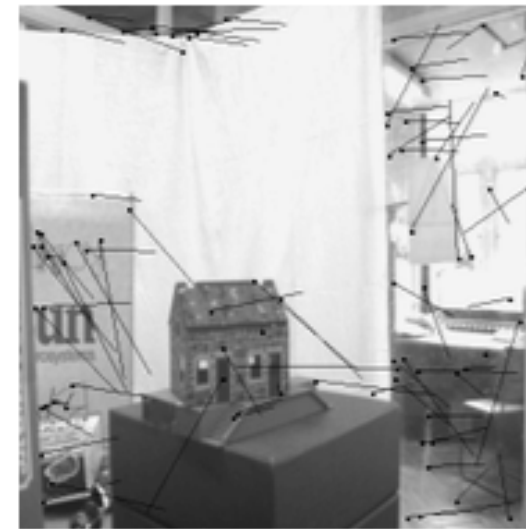
(c)



(d)

Figure 7: Indoor sequence, camera translating and rotating while fixated on the model house: (a) first image, (b) second image, (c) matches, (d) inliers, and (e) outliers. The data are found to be degenerate with respect to the fundamental matrix.

Figure 7 shows a scene in which a camera rotates and translates whilst fixating on a model house. The important thing about this image pair is that the structure recovery for this image pair proved highly unstable. The reason for this instability is not immediately apparent until the good fit of the quadratic transformation is witnessed, indicating that the structure is close to a critical surface.



(e)

## Points and Epipolar geometry: Fundamental Matrix: ambiguous solutions

Torr, Zisserman, & Maybank 1996, “Robust Detection of Degenerate Configurations whilst Estimating the Fundamental Matrix <https://www.robots.ox.ac.uk/~phst/Papers/CVIU97/m.ps.gz>



(a)



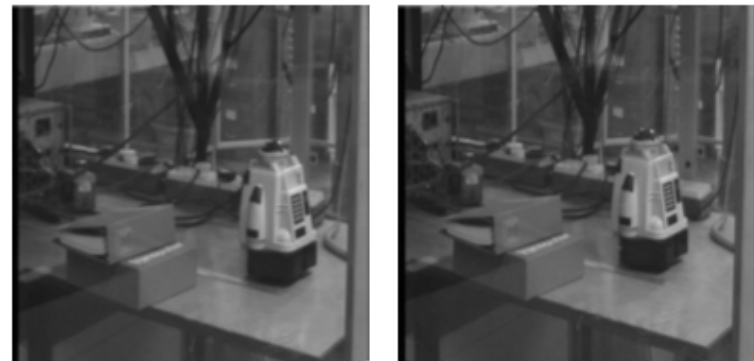
(b)

Figure 8: Indoor sequence, camera translating and rotation to fixate on the house. (a) left image, (b) right image and inliers.

The scene is correctly flagged as a general motion, as the translation and rotational components of the camera motion were both significant, and full perspective structure can be recovered.

## Points and Epipolar geometry:Fundamental Matrix: ambiguous solutions

**Torr, Zisserman, & Maybank 1996, “Robust Detection of Degenerate Configurations whilst Estimating the Fundamental Matrix** <https://www.robots.ox.ac.uk/~phst/Papers/CVIU97/m.ps.gz>



(a)



(b)



(c)



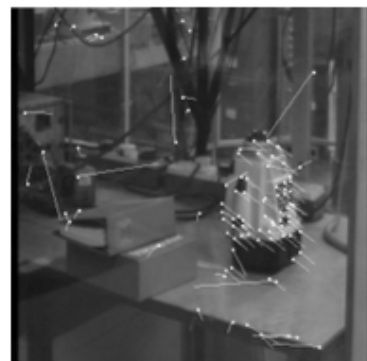
(d)



(e)



(f)



(g)

Figure 9: (a) first image, (b) second image, (c) matches of the sequence with an independently moving robot viewed from a camera, translating vertically down (parallel to the image plane). The robot moves along the table. Fundamental matrix inliers (d) and outliers (e) for F. It can be seen that the independently moving robot is not fully segmented. PLUNDER.DL indicated an affinity fit, with inliers (f) and outliers (g). The independently moving robot is fully segmented.

The scene contains an independently moving robot. The correspondences are shown in (c). The aim is to cluster all the points consistent with the background whilst excluding points on the robot and outliers. To demonstrate the advantage of the new degeneracy detection algorithm we compare our results with those obtained from a more conventional robust estimator, RANSAC. Figure 9 (d) shows the inliers and Figure 9 (e) shows the outliers predicted using a full fundamental matrix estimated by RANSAC. It can be seen in (d) that not all the points on the robot are flagged as inconsistent with the background. However, the PLUNDER.DL selected model (an affinity) does eliminate these matches.

# Points and Epipolar geometry:Fundamental Matrix: cheirality

Wei Xu and J. Mulligan,

“Robust relative pose estimation with integrated cheirality constraint,” *2008 19th International Conference on Pattern Recognition, Tampa, FL, USA, 2008*, pp. 1-4, doi: 10.1109/ICPR.2008.4761509.

<https://citeseerx.ist.psu.edu/viewdoc/download?doi=10.1.1.194.2538&rep=rep1&type=pdf>

1. Compute feature correspondences between two images taken from different viewpoints.
2. Repeat for n hypothesis-and-test trials. In each trial do the following:
  1. (a) Select a random sample of the minimum number of correspondences; use a hypothesis generator to generate a hypothesis of the epipolar geometry ( $F$  or  $E$ );
  2. (b) Check the cheirality of the sample points. If points disagree on cheirality discard hypothesis, goto (a). Otherwise record the cheirality of the sample/hypothesis CH.
  3. (c) Reconstruct *all the correspondences* and for each reconstructed point compute the reprojection error:  $e2_i = i(d(p1, p^1)^2 + d(p2, p^2)^2)$  where  $d$  is the Euclidean distance in the image between the original correspondence points  $(p1, p2)$  and the projections of the reconstructed point  $(\hat{p}1, \hat{p}2)$ .
  4. (d) Count the number of points with distance  $e_i$  less than some threshold  $T$ . These points are regarded as inliers consistent with the epipolar geometry hypothesis.
  5. (e) For each inlier, we check its cheirality  $C_i$ . If  $C_i = CH$ , it's an inlier consistent with the hypothesis in both epipolar geometry and cheirality. Record the number of cheirality-verified inliers.
3. Select the largest refined inlier set consistent with its generating hypothesis in both epipolar geometry and cheirality.
4. Use all the refined inliers to re-estimate the epipolar geometry ( $F$  or  $E$ ).
5. Derive  $E$  from  $F$  (if necessary), and re-compute the relative motion  $[R, t]$  from the re-estimated  $E$ .

popular epipolar geometry framework. For generality considerations, we use Nister’s approach [7] to evaluate the cheirality of the correspondences. Given an estimated  $E$ , the cheirality  $C_i$  of a correspondence has four possible configurations:  $[R_a|t_u]$ ,  $[R_a|-t_u]$ ,  $[R_b|t_u]$  and  $[R_b|-t_u]$  where  $R_a = UDV^T$  and  $R_b = UD^TV^T$ ;  $[U, \Sigma, V] = svd(E)$  with  $\det(U) > 0$  and  $\det(V) > 0$ ;  $D$  is a predefined matrix and  $t_u$  is the third column of  $U$ .

[7] D. Nister. An efficient solution to the five-point relative pose problem. In Proc. 2003 IEEE Computer Society Conference on Computer Vision and Pattern Recognition(CVPR’03), volume 2, pages 195–202, June 2003

## Points and Epipolar geometry: Fundamental Matrix: cheirality

D. Nister. An efficient solution to the five-point relative pose problem. In Proc. 2003 IEEE Computer Society Conference on Computer Vision and Pattern Recognition(CVPR'03), volume 2, pages 195–202, June 2003

The uncalibrated methods fail when faced with coplanar scene points, since there is then a continuum of possible solutions.

In the calibrated setting, coplanar scene points only cause at most a two-fold ambiguity [15, 17]. With a third view, the ambiguity is in general resolved.

chirality constraint: scene points should be in front of the cameras

Image points are represented by homogeneous 3-vectors  $q$  and  $q'$  in the first and second view, respectively. World points are represented by homogeneous 4-vectors  $Q$ . A per-

Any combination of  $R$  and  $t$  according to the above prescription satisfies the epipolar constraint (4). To resolve the inherent ambiguities, it is assumed that the first camera matrix is  $[I \mid 0]$  and that  $t$  is of unit length. There are then the following four possible solutions for the second camera matrix:  $P_A \equiv [R_a \mid t_u]$ ,  $P_B \equiv [R_a \mid -t_u]$ ,  $P_C \equiv [R_b \mid t_u]$ ,  $P_D \equiv [R_b \mid -t_u]$ . One of the four choices corresponds to the true configuration. Another one corresponds to the twisted pair which is obtained by rotating one of the views 180 degrees around the baseline. The remaining two correspond to reflections of the true configuration and the twisted pair. For example,  $P_A$  gives one configuration.  $P_C$  corresponds to its twisted pair, which is obtained by applying the transformation

$$H_t \equiv \begin{bmatrix} I & 0 \\ -2v_{13} & -2v_{23} & -2v_{33} & -1 \end{bmatrix}. \quad (22)$$

$P_B$  and  $P_D$  correspond to the reflections obtained by applying  $H_r \equiv \text{diag}(1, 1, 1, -1)$ . In order to determine which choice corresponds to the true configuration, the chirality constraint <sup>1</sup> is imposed. One point is sufficient to resolve the ambiguity. The point is triangulated using the view pair  $([I \mid 0], P_A)$  to yield the space point  $Q$  and chirality is tested. If  $c_1 \equiv Q_3 Q_4 < 0$ , the point is behind the first camera. If  $c_2 \equiv (P_A Q)_3 Q_4 < 0$ , the point is behind the second camera. If  $c_1 > 0$  and  $c_2 > 0$ ,  $P_A$  and  $Q$  correspond to the true configuration. If  $c_1 < 0$  and  $c_2 < 0$ , the reflection  $H_r$  is applied and we get  $P_B$ . If on the other hand  $c_1 c_2 < 0$ , the twist  $H_t$  is applied and we get  $P_C$  and the point  $H_t Q$ . In this case, if  $Q_3 (H_t Q)_4 > 0$  we are done. Otherwise, the reflection  $H_r$  is applied and we get  $P_D$ .

Points and Epipolar geometry: Fundamental Matrix: cheirality

chirality constraint: scene points should be in front of the cameras

**R. Hartley. Cheirality invariants. In DARPA'93, pages 745–753, 1993.**

<https://citeseerx.ist.psu.edu/viewdoc/download?doi=10.1.1.49.4493&rep=rep1&type=pdf>

from “Multiple View Geometry in Computer Vision”

Second Edition by Hartley & Zisserman

<https://www.robots.ox.ac.uk/~vgg/hzbook/code/>

(Note, consult author and book for any of this. use it's presented here for educational purposes only.)

see vgg\_multiview/vgg\_F\_from\_7pts\_2img.m:50:function OK

## multi-view geometry

With point correspondences  $\mathbf{m}_i \longleftrightarrow \mathbf{M}_i$ , can solve for camera projection matrix P. Using the Kroenecker delta product and vec operator, coefficients are rewritten to their linearly independent forms of a matrix of size  $2n \times 12$  called the coefficient matrix A

From a set of n point correspondences, we obtain a  $2n \times 12$  coefficient matrix A, where n must be  $> 6$ .

In general A will have rank 11 (provided that the points are not all coplanar) and the solution is the *1-dimensional right null-space of A*.

The linear system of equations for inexact data is solved using least squares.

The least-squares solution for  $\text{vec } \mathbf{P}^T$  is the singular vector corresponding to the smallest *singular value* decomposition of A and the direct linear transform.

The equation is usually written in form  $A * h = 0$  where h is  $\text{vec } \mathbf{P}^T$  (its the one dimensional reshaping of the homograph matrix).



## multi-view geometry (cont.)

In general:

- dot product of a point and a line is zero if the point lies on the line
- if the *intrinsic parameters* are known, the relationship between corresponding points is given by the *essential matrix*:  $\mathbf{m}_r^T * \mathbf{E} * \mathbf{m}_l^T$
- when no camera details are available, one can use the *fundamental matrix*.

It's a  $3 \times 3$  rank 2 homogeneous matrix. It has 7 degrees of freedom.

For any point  $\mathbf{m}_l$  in the left image, the corresponding epipolar line  $\mathbf{l}_r$  in the right image can be expressed as  $\mathbf{l}_r = \mathbf{F} * \mathbf{m}_l$  and vice versa  $\mathbf{l}_r = \mathbf{F}^T * \mathbf{m}_r$

- the *essential and fundamental matrices* are related through  $\mathbf{F} = \mathbf{K}_r^{-T} * \mathbf{E} * \mathbf{K}_l^{-T}$  where  $\mathbf{K}_r$  and  $\mathbf{K}_l$  are the left and right camera matrices

Regarding 3D reconstruction:

- when both *intrinsic* and *extrinsic* camera parameters are known, the reconstruction is solved unambiguously by triangulation.
- when only *intrinsic* parameters are known, extrinsic parameters can be estimated and the reconstruction can be solved up to an unknown scale factor, that is  $\mathbf{R}$  can be estimated, but  $\mathbf{t}$  can be only up to a scale factor. the epipolar geometry is the essential matrix and the solvable projection is euclidean (rigid+ uniform scale)
- when neither *intrinsic* nor *extrinsic* parameters are known, i.e., the only information available are pixel correspondences, the reconstruction can be solved up to an unknown, global projective transformation of the world.

In Trifocal geometry, a trifocal tensor is used.

## Statistics of matching correspondence: Fundamental Matrix

from “IVPV Handbook of Optics”, Vol II  
edited by Michael Bass  
[http://photonics.intec.ugent.be/  
education/IVPV/res\\_handbook/  
v2ch17.pdf](http://photonics.intec.ugent.be/education/IVPV/res_handbook/v2ch17.pdf)

from “Multiple View Geometry in Computer Vision”  
Second Edition by Hartley & Zisserman  
<https://www.robots.ox.ac.uk/~vgg/hzbook/>

(Note, consult authors and books for any use.)

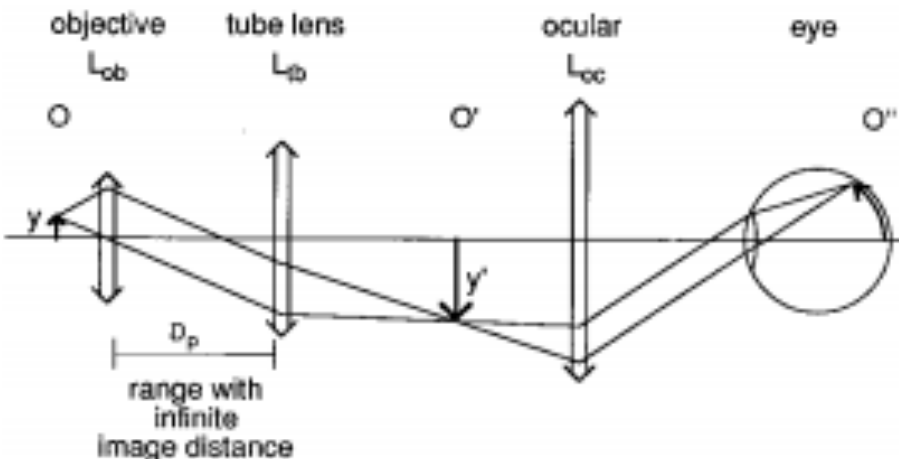


**FIGURE 4** Ray path in microscope with infinity-corrected objective and tube lens.

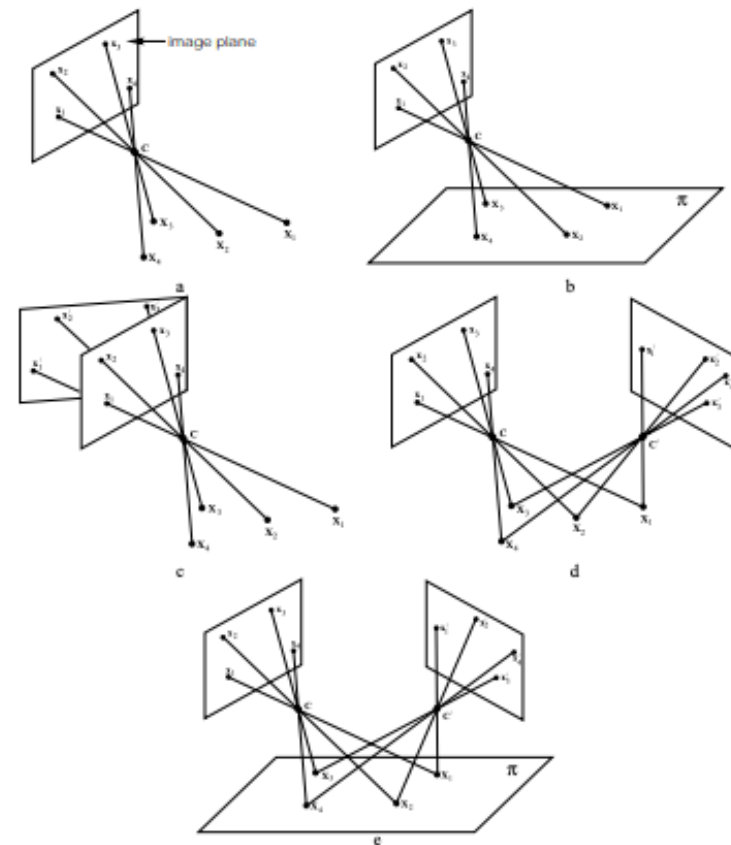


**Fig. 1.1. The camera centre is the essence.** (a) Image formation: the image points  $x_i$  are the intersection of rays from the space points  $X_i$  through the camera centre C. (b) If the space points are coplanar then there is a projective transformation between the world and image planes,  $x'_i = H_{3 \times 3}x_i$ . (c) All images with the same camera centre are related by a projective transformation,  $x'_i = H'_{3 \times 3}x_i$ . Compare (b) and (c) – in both cases planes are mapped to one another by rays through a centre. In (b) the mapping is between a scene and image plane, in (c) between two image planes. (d) If the camera centre moves, then the images are in general not related by a projective transformation, unless (e) all the space points are coplanar.

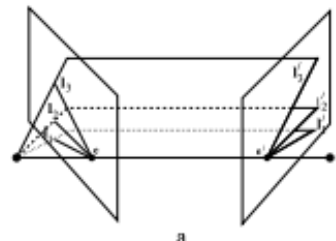
from “Multiple View Geometry in Computer Vision”

Second Edition by Hartley & Zisserman

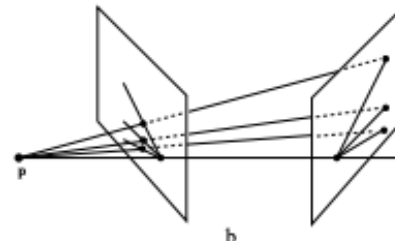
<https://www.robots.ox.ac.uk/~vgg/hzbook/>

(Note, consult author and book for any of this. use it's presented here for educational purposes only.)

9.3 Fundamental matrices arising from special motions



a



b

Fig. 9.6. Epipolar line homography. (a) There is a pencil of epipolar lines in each image centred on the epipole. The correspondence between epipolar lines,  $l_i \leftrightarrow l'_i$ , is defined by the pencil of planes with axis the baseline. (b) The corresponding lines are related by a perspectivity with centre any point  $p$  on the baseline. It follows that the correspondence between epipolar lines in the pencils is a 1D homography.

247

246

### 9 Epipolar Geometry and the Fundamental Matrix

- $F$  is a rank 2 homogeneous matrix with 7 degrees of freedom.
- **Point correspondence:** If  $x$  and  $x'$  are corresponding image points, then  $x'^T F x = 0$ .
- **Epipolar lines:**
  - $l' = Fx$  is the epipolar line corresponding to  $x$ .
  - $l = F^T x'$  is the epipolar line corresponding to  $x'$ .
- **Epipoles:**
  - $F e = 0$ .
  - $F^T e' = 0$ .
- **Computation from camera matrices  $P, P'$ :**
  - General cameras,  $F = [e'] \times P' P^+$ , where  $P^+$  is the pseudo-inverse of  $P$ , and  $e' = P' C$ , with  $P C = 0$ .
  - Canonical cameras,  $P = [I \mid 0]$ ,  $P' = [M \mid m]$ ,  $F = [e'] \times M = M^{-T} [e] \times$ , where  $e' = m$  and  $e = M^{-1} m$ .
  - Cameras not at infinity  $P = K[I \mid 0]$ ,  $P' = K'[R \mid t]$ ,  $F = K'^{-T} [t] \times R K^{-1} = [K't] \times K'R K^{-T} = K'^{-T} R K^T [K'R^T t] \times$ .

Table 9.1. Summary of fundamental matrix properties.

## Bundle Adjustment

from “Bundle Adjustment — A Modern Synthesis”

by Triggs, McLauchlan, Hartley, and Fitzgibbon

Vision Algorithms’99, LNCS 1883, pp. 298–372, 2000

<http://www.cs.jhu.edu/~misha/ReadingSeminar/Papers/Triggs00.pdf>

(Note, consult author for any use of figures and text - it’s presented here for educational purposes only.)

(not implemented in this project currently)

Bundle adjustment: refining a visual reconstruction to produce jointly optimal 3D structure and viewing parameter (camera pose and/or calibration) estimates, by minimizing a cost function that quantifies the model fitting error, and jointly that the solution is simultaneously optimal with respect to both structure and camera variations... a large sparse geometric parameter estimation problem, the parameters being the combined 3D feature coordinates, camera poses and calibrations.

cost function: often use non-quadratic M-estimator-like distributional models to handle outliers more integrally, and many include additional penalties related to overfitting, model selection and system performance (priors, MDL).

modelled as a sum of opaque contributions from the independent information sources (individual observations, prior distributions, overfitting penalties ... ). The functional forms of these contributions and their dependence on fixed quantities such as observations will usually be left implicit

main conclusion will be that robust statistically-based error metrics based on total (inlier + outlier) log likelihoods should be used, to correctly allow for the presence of outliers... A typical ML cost function would be the *summed negative log likelihoods* of the prediction errors of all the observed image features. For Gaussian error distributions, this reduces to the *sum of squared covariance-weighted prediction errors* (§3.2). A MAP estimator (is Bayesian) would typically add cost terms giving certain structure or camera calibration parameters a bias towards their expected values.

first realize that geometric fitting is really a special case of parametric probability density estimation.

Maximizing the likelihood corresponds to fitting this predicted observation density to the observed data. The geometry and camera model only enter indirectly, via their influence on the predicted distributions.

ML estimation is naturally robust to outliers.

## Bundle Adjustment

from “Bundle Adjustment — A Modern Synthesis”

by Triggs, McLauchlan, Hartley, and Fitzgibbon

Vision Algorithms’99, LNCS 1883, pp. 298–372, 2000

<http://www.cs.jhu.edu/~misha/ReadingSeminar/Papers/Triggs00.pdf>

(Note, consult author for any use of figures and text - it’s presented here for educational purposes only.)

### Pattern Matrices and Factorization:

The most common **top-down** method is called nested dissection or recursive partitioning: recursively split the factorization problem into smaller sub-problems, solve these independently, and then glue the solutions together along their common boundaries. Splitting involves choosing a separating set of variables, whose deletion will separate the remaining variables into two or more independent subsets. This corresponds to finding a (vertex) graph cut of the elimination graph, i.e. a set of vertices whose deletion will split it into two or more disconnected components.

Given such a partitioning, the variables are reordered into **connected components**, with the separating set ones last. This produces a pattern matrix such as ‘block tridiagonal matrix’, ‘arrowhead matrix’, or ‘bundle hessian’, etc.

\*\*Finding a globally minimal partition sequence is NP complete but several effective heuristics exist.

Many **bottom-up** variable ordering heuristics exist.

Deciding the reconstructed coordinate system is in the realm of **Gauge Freedom** (a gauge is a reference frame):

constraining the coordinate values of certain aspects of the reconstructed structure — features, cameras or combinations of these — whatever the rest of the structure might be.

## Bundle Adjustment

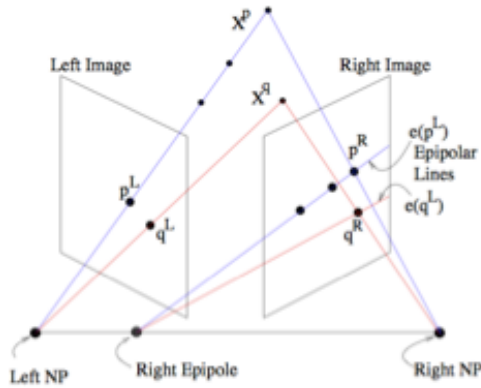
from “Bundle Adjustment in the Large”, 2010  
by Agarwal, Snavely, Seitz, and Szeliski

<https://homes.cs.washington.edu/~sagarwal/bal.pdf>

(Note, consult author for any use of figures and text - it's presented here for educational purposes only.)

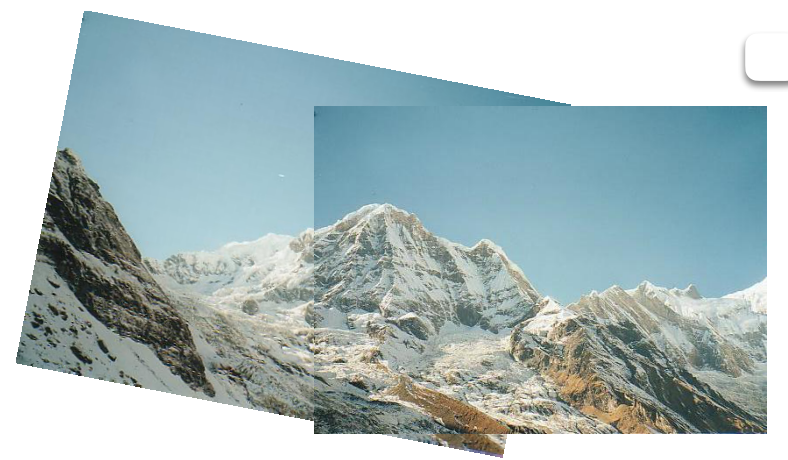
treated as re-weighted non-linear least squares problem .

## Projection, stereo and panoramic images



<http://www.cs.toronto.edu/~jepson/csc420/notes/epiPolarGeom.pdf>  
(note, the image is posted on an educational site and copied here without following up on permissions. Any further use of the image should follow up on the origins and permissions.)

**panoramic** images here are from  
Brown & Lowe 2003



## rectification and registration

from “Computing Rectifying Homographies for

### Stereo Vision”

by Loop & Zhang, 1999

<https://www.microsoft.com/en-us/research/wp-content/uploads/2016/02/tr99-21.pdf>

the transforms  $H_p$  and  $H_{0p}$  were found that map the epipoles  $e$  and  $e_0$  to points at 1. In this section we define a pair of similarity transforms  $H_r$  and  $H_{0r}$  that rotate these points at inf. into alignment with the direction  $i = [1 \ 0 \ 0]^T$  as required for rectification. Additionally, a translation in the v-direction on one of the images is found to exactly align the scan-lines in both images.

... reduce the distortion with a shearing transform.

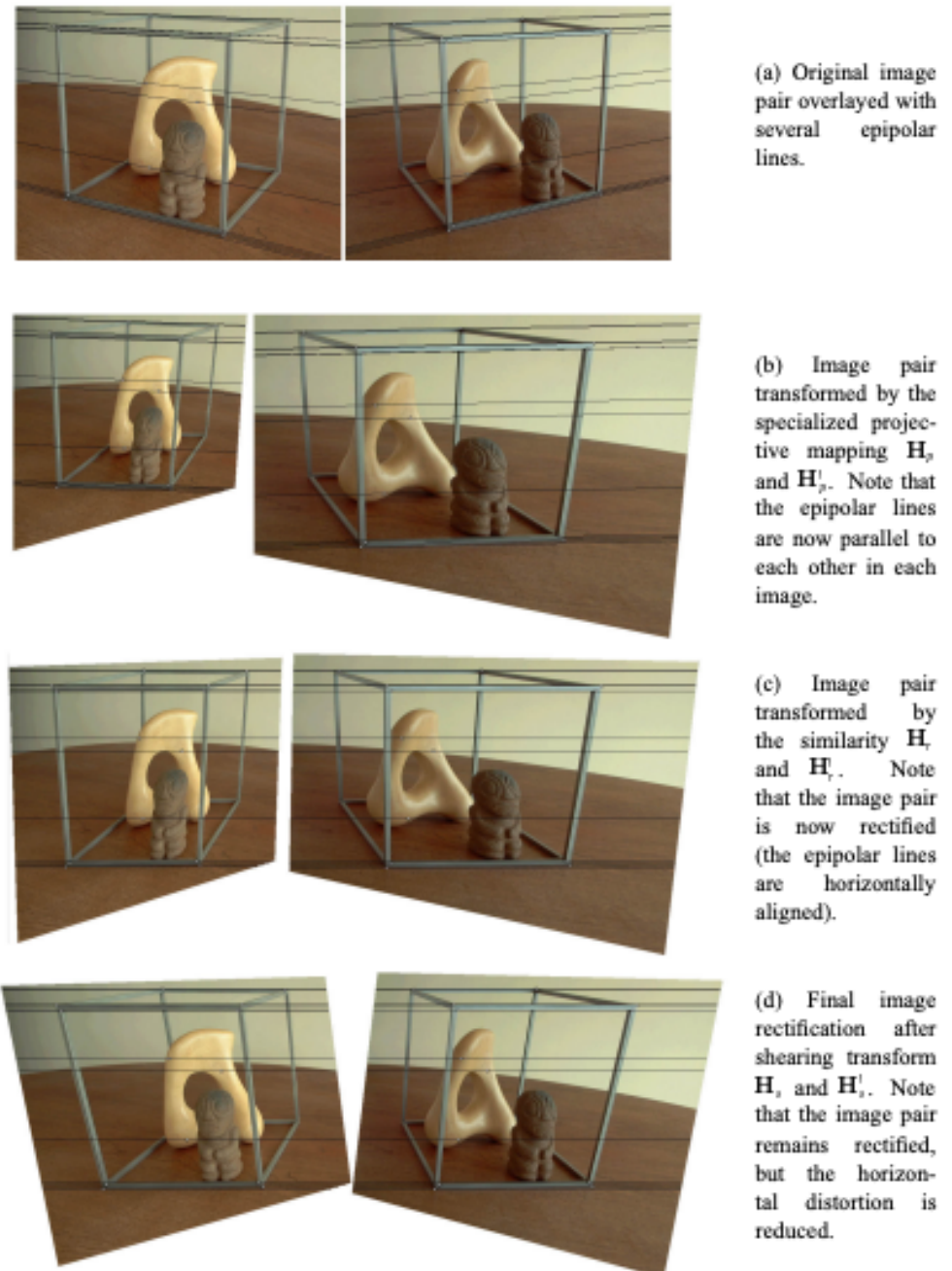


Figure 3: An example showing various stages of the proposed rectification algorithm.

## Projection, stereo and panoramic images

A review on bundle adjustment and 3D rectification and tracking in Section 1 and 2 of this paper:  
(not implemented in this project)

from “Flight Dynamics-based Recovery of a UAV Trajectory using Ground Cameras”

by Rozantsev et al. 2017

[http://openaccess.thecvf.com/content\\_cvpr\\_2017/papers/Rozantsev\\_Flight\\_Dynamics-Based\\_Recovery\\_CVPR\\_2017\\_paper.pdf](http://openaccess.thecvf.com/content_cvpr_2017/papers/Rozantsev_Flight_Dynamics-Based_Recovery_CVPR_2017_paper.pdf)

We propose a new method to estimate the 6-dof trajectory of a flying object such as a quadrotor UAV within a 3D airspace monitored using multiple fixed ground cameras...Our method requires neither perfect single-view tracking nor appearance matching across views. For robustness, we allow the tracker to generate multiple detections per frame in each video. The true detections and the data association across videos is estimated using robust multi-view triangulation and subsequently refined during our bundle adjustment procedure.



...

existing multi-camera tracking methods are designed to track people, vehicles to address indoor and outdoor surveillance tasks, where the targets are often on the ground. In contrast, small drones must be tracked within a 3D volume that is orders of magnitude larger

...

Most existing multi-camera systems also rely on accurate camera calibration that requires someone to collect calibration data by walking around in the scene.

...

## 3D from structured light

active sensing method called phase shifting method (PSM)  
(not implemented in this project)



**single point perspective and two and three point perspectives** sometimes can have “foreshortened” object dimensions if the axes of the object are not parallel to the camera plane.

For example, when creating correspondence for the gingerbread man in the image below using partial shape matching and euclidean transformation for evaluation, half of the object is unmatched within a tolerance.

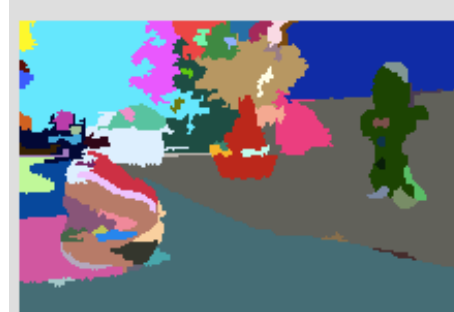
So, a rough calculation of the angle of inclination is needed to find the other matching points consistent with a single-point perspective projection.

The “foreshortening” along the x-axis is corrected using cosine of the angle, that is the true dimension is the measured divided by cosine of angle.

The foreshortening along the y axis can be approximated by the ratio of the far sides of two triangles, one embedded in the other.



*image for the search for  
gingerbread man*

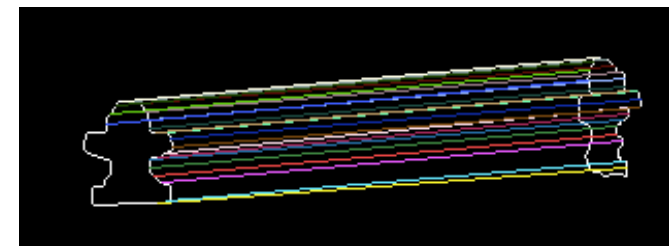


*segmentation*

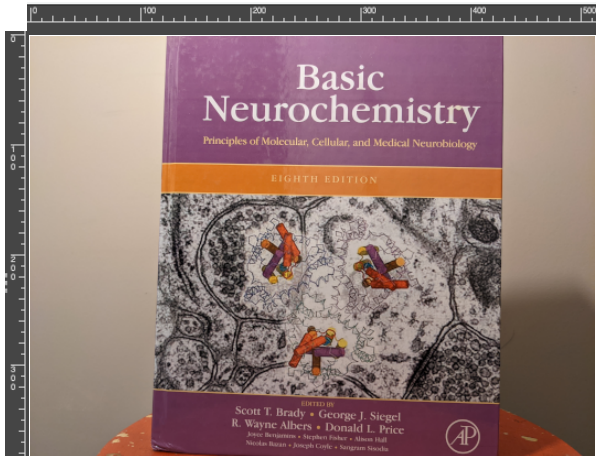


***segmentation filtered to  
colors similar to the  
template object  
gingerbread man (not  
shown)***

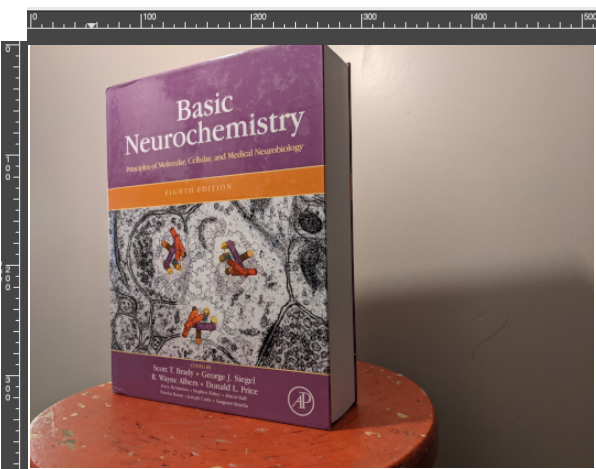
***euclidean transformed matches  
...need a perspective projection  
search for the other half***



## SVD and epipolar details on test images



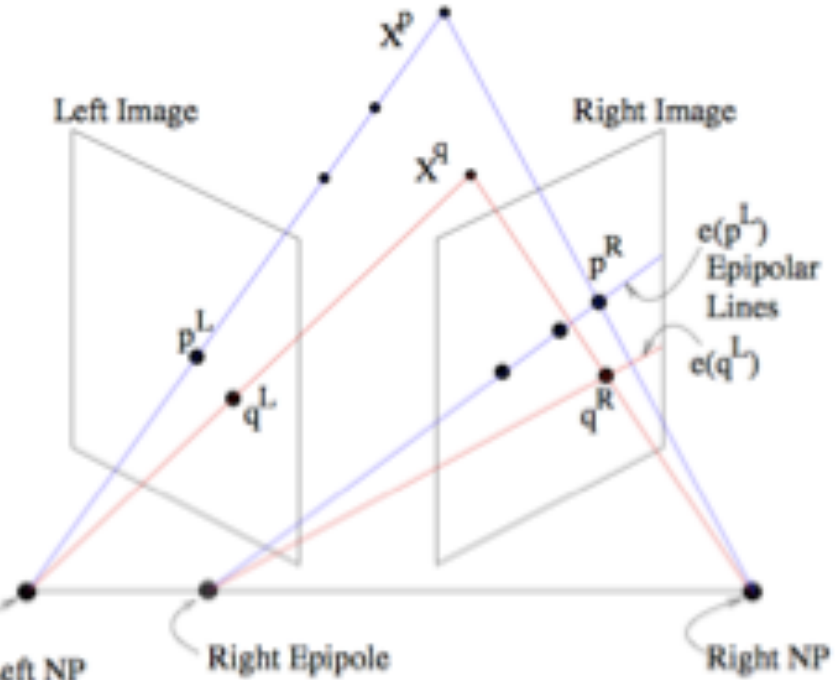
**Coords:**  
 262, 356  
 316, 342  
 260, 305  
 284, 279  
 234, 217  
 177, 76  
 216, 63  
 220, 158



**Coords:**  
 156, 308  
 191, 301  
 153, 270  
 167, 249  
 135, 202  
 97, 97  
 119, 83  
 125, 156

pixel width = 1.4e-3mm  
 image dimensions originally 4032x3024,  
 then divided by 7.875 to 512x384, 300 dpi  
 FOV = 77 degrees = 1.344 radians  
 focal length = (4032/2.) / tan(1.344/2.)  
 ~ 1604 pixels = 2.245 mm

not yet including software scaling or  
 magnification of image by camera components  
 (figuratively by lens to world system)

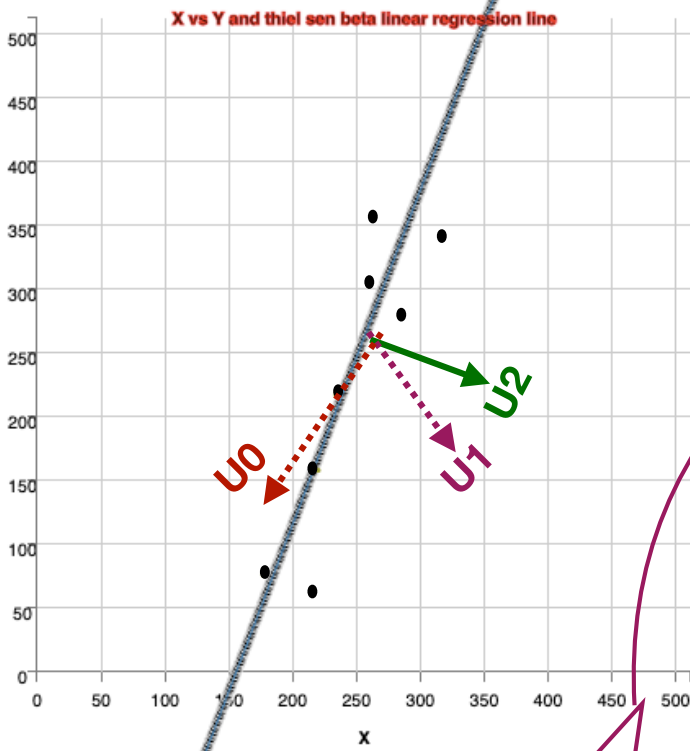


intrinsic camera matrix

$$K = \begin{vmatrix} 1604 & 0 & 2016 \\ 0 & 1604 & 1512 \\ 0 & 0 & 1 \end{vmatrix}$$

## SVD and epipolar details on test images

**img1:**



$u_0 = [-0.7077/0.0027, -0.7065/0.0027, 1]$   
 $= [-262.1, -261.7, 1]$   
 $\Rightarrow u_0 \text{ theta} = 45 \text{ degrees}$   
 $u_1 = [0.7065/0.0049, -0.7077/0.0049, 1]$   
 $= [144.2, -144.4, 1]$   
 $\Rightarrow u_1 \text{ theta} = -45 \text{ degrees}$

Coords:

$X =$   
 262.000 , 316.000 , 260.000 284.000 234.000 177.000 216.000 220.000  
 356.000 , 342.000 , 305.000 279.000 217.000 76.000 63.000 158.000  
 1.000 , 1.000 , 1.000 1.000 1.000 1.000 1.000 1.000  
 mean=246.1250, 224.5000, 1.0000  
 stDev=43.5511, 115.3640, 0.0000

thiel sen y-Intercept, slope = (-407.64, 2.62)

SVD(X):

$U =$   
 $-0.7077, 0.7065, -0.0054$   
 $-0.7065, -0.7077, 0.0015$   
 $-0.0027, 0.0049, 1.0000$

$u_2 \text{ theta} = \text{atan}(0.0015/-0.0054)$   
 vector x and y lengths scaled by 100  
 $= (100*\cos(\theta), 100*\sin(\theta))$   
 $= (96.35, -26.76)$   
 drawn relative to (256, 256) in plot

$S = [984.6910338036112, 157.01103159470784, 0.3223419627696029]$

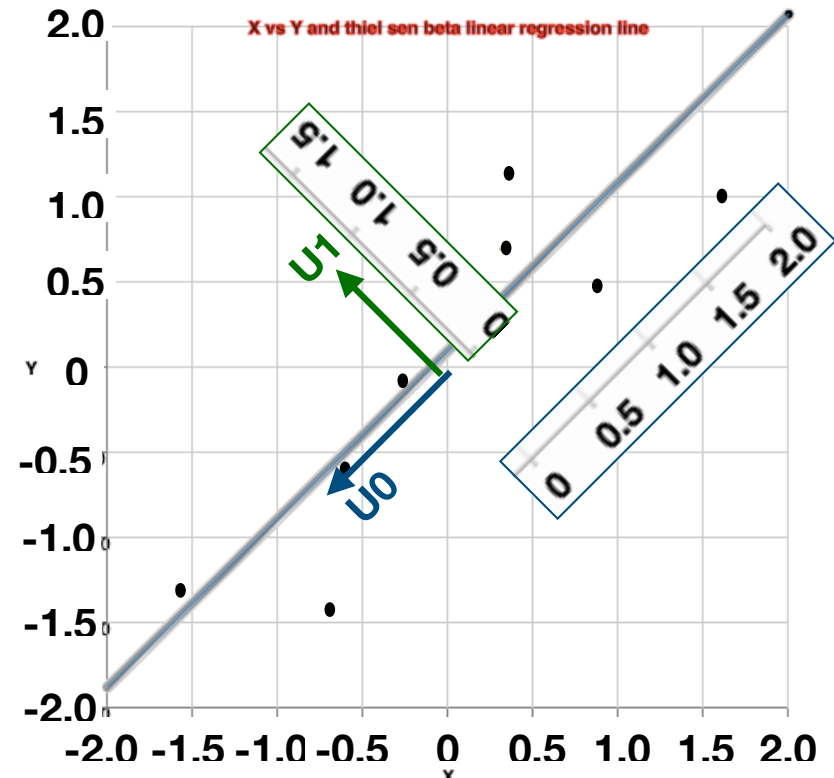
$V^T =$

$-0.4437, -0.4725, -0.4057, -0.4043, -0.3239, -0.1817, -0.2004, -0.2715$   
 $-0.4256, -0.1195, -0.2047, 0.0205, 0.0749, 0.4539, 0.6880, 0.2778$   
 $0.3909, -0.5772, 0.1854, -0.3374, 0.2078, 0.5001, -0.2126, 0.1655$   
 $-0.3909, -0.4000, 0.3803, 0.6804, -0.0498, 0.0988, -0.2504, -0.0684$   
 $-0.3261, 0.0470, -0.0843, -0.1033, 0.8999, -0.1365, -0.1738, -0.1229$   
 $-0.2312, 0.4917, -0.0691, -0.0872, -0.1348, 0.6723, -0.4115, -0.2302$   
 $-0.2634, 0.0864, 0.7687, -0.4571, -0.0758, -0.0770, 0.2452, -0.2271$   
 $-0.2955, 0.1337, 0.1083, -0.1792, -0.1008, -0.1568, -0.3448, 0.8351$

**NOTE:** naively, one can see here and on next page that using geometric median in an **alternative normalization** would require adjustments in use of SVD analysis.

## SVD and epipolar details on test images

### img1 after standard normalization:



Normalized Coords:

$A = X =$   
 $\begin{bmatrix} 0.365 & 1.604 & 0.319 & 0.870 & -0.278 & -1.587 & -0.692 & -0.600 \\ 1.140 & 1.019 & 0.698 & 0.472 & -0.065 & -1.287 & -1.400 & -0.576 \end{bmatrix}$   
 mean=0,0; stDev=1,1

thiel sen y-Intercept, slope = (10.2, 0.99)

SVD(Normalized X w/ dimension reduction):

$U =$   
 $\begin{bmatrix} -0.7071 & -0.7071 \\ -0.7071 & 0.7071 \end{bmatrix}$

$S = [3.613605578424382, 0.9704920007811456]$

$V^T =$

$\begin{bmatrix} -0.2944 & -0.5133 & -0.1989 & -0.2626 & 0.0672 & 0.5625 & 0.4093 & 0.2302 \\ 0.5649 & -0.4269 & 0.2763 & -0.2894 & 0.1555 & 0.2186 & -0.5160 & 0.0171 \\ -0.3131 & 0.0857 & 0.9273 & -0.0291 & -0.0009 & 0.1034 & 0.1443 & 0.0497 \\ -0.0304 & -0.4073 & 0.0581 & 0.8962 & 0.0490 & 0.1115 & -0.1051 & 0.0257 \\ -0.0399 & 0.1690 & -0.0341 & 0.0347 & 0.9812 & -0.0254 & 0.0637 & -0.0016 \\ 0.3001 & 0.5531 & -0.0299 & 0.1822 & -0.0742 & 0.7458 & 0.0437 & -0.0795 \\ 0.6135 & -0.1346 & 0.1373 & 0.0652 & -0.0022 & -0.2108 & 0.7268 & -0.0991 \\ 0.1652 & 0.1688 & 0.0048 & 0.0673 & -0.0248 & -0.1068 & -0.0148 & 0.9630 \end{bmatrix}$

for  $i \leq \text{rank}$ ,  $A^* v_i = \sigma u_i$   
 (for  $i > \text{rank}$ ,  $A^* v_i = 0$  and  $A^T u_i = 0$ )

$U_0 * S_0 = [-2.555, -2.555]$

$U_1 * S_1 = [-0.686, 0.686]$

$A * V =$

$\begin{bmatrix} -2.555 & -0.686 & -0.000 & -0.000 & -0.000 & 0.000 & 0.000 & 0.000 \\ -2.555 & 0.686 & 0.000 & -0.000 & -0.000 & 0.000 & 0.000 & 0.000 \end{bmatrix}$

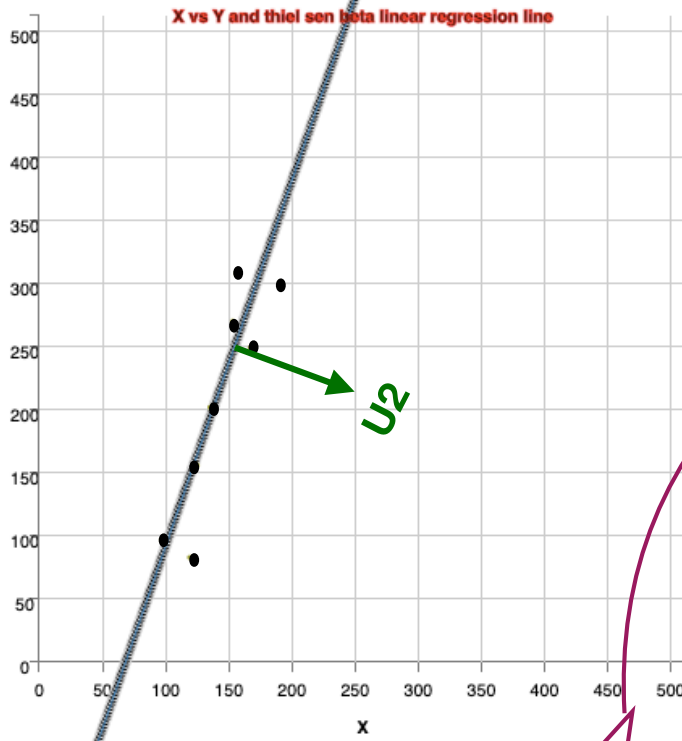
$A * v_0 = [-2.555, -2.555]$

$a^T * u_0 = [-1.064, -1.855, -0.719, -0.949, 0.243, 2.033, 1.479, 0.832]$

$a^T * u_1 = [0.548, -0.414, 0.268, -0.281, 0.151, 0.212, -0.501, 0.017]$

## SVD and epipolar details on test images

**img2:**



$u_0 = [-0.5408/-0.0036, -0.8412/-0.0036, 1]$   
 $= [150.2, 233.7, 1]$   
 $\Rightarrow u_0 \text{ theta} = 57 \text{ degrees}$   
 $u_1 = [0.8411/0.0102, -0.5408/0.0102, 1]$   
 $= [82.5, -53, 1]$   
 $\Rightarrow u_1 \text{ theta} = -32.7 \text{ degrees}$

**Coords:**

$X =$   
 156.000 , 191.000 , 153.000 167.000 135.000 97.000 119.000 125.000  
 308.000 , 301.000 , 270.000 249.000 202.000 97.000 83.000 156.000  
 1.000 , 1.000 , 1.000 1.000 1.000 1.000 1.000 1.000  
 mean=142.8750, 208.25, 1.0000  
 stDev=29.8302, 88.5272, 0.0000

thiel sen y-Intercept, slope = (-197.4, 2.9)

SVD(X) :

$U =$   
 $-0.5408, 0.8411, -0.0105$   
 $-0.8412, -0.5408, 0.0025$   
 $-0.0036, 0.0102, 0.9999$   
 $S = [751.94, 77.04, 0.41]$

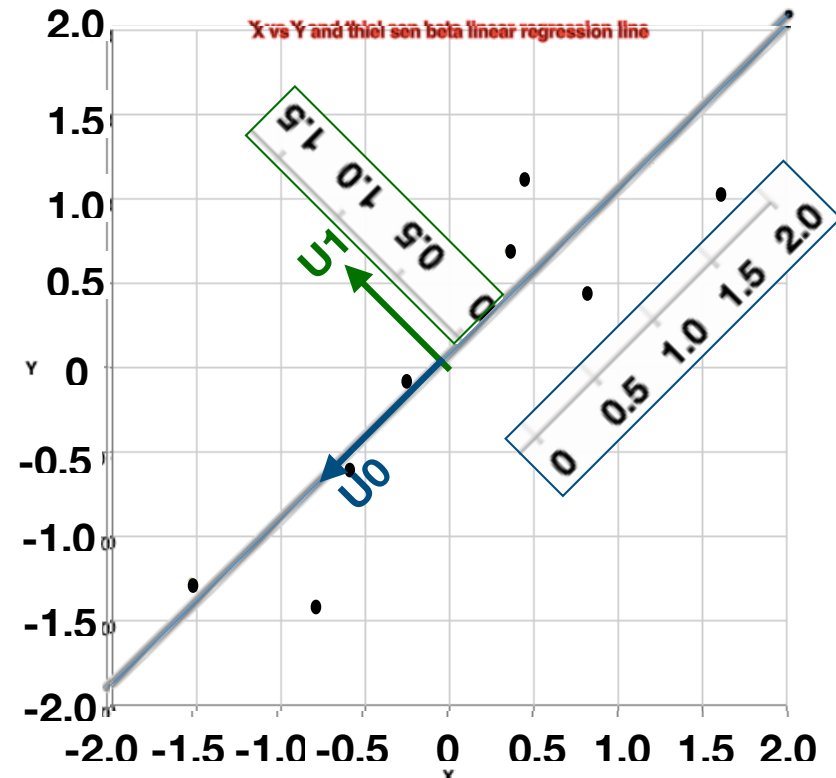
$u_2 \text{ theta} = \text{atan}(0.0025/-0.0105)$   
 vector x and y lengths scaled by 100  
 $= (100*\cos(\theta), 100*\sin(\theta))$   
 $= (97.3, -23.2)$   
 drawn relative to (256, 256) in plot

$V^T =$

$-0.4567, -0.4741, -0.4121, -0.3987, -0.3231, -0.1783, -0.1784, -0.2644$   
 $-0.4586, -0.0273, -0.2246, 0.0756, 0.0562, 0.3783, 0.7167, 0.2699$   
 $0.3257, -0.6127, 0.1700, -0.3167, 0.2146, 0.5447, -0.1038, 0.1891$   
 $-0.0066, -0.4255, -0.2453, 0.8435, 0.0139, 0.0590, -0.2061, -0.0329$   
 $-0.3923, -0.0698, 0.1100, -0.0394, 0.8647, -0.2144, -0.1157, -0.1431$   
 $-0.4748, 0.0728, 0.6221, 0.1278, -0.2574, 0.4116, -0.2046, -0.2973$   
 $0.1439, -0.4350, 0.4627, 0.0737, -0.1031, -0.4470, 0.5484, -0.2436$   
 $-0.2738, -0.1367, 0.2784, 0.0151, -0.1469, -0.3313, -0.2124, 0.8076$

## SVD and epipolar details on test images

### img2 after standard normalization:



Normalized Coords:

$A = X =$   
 $\begin{matrix} 0.440 & , & 1.613 & 0.339 & 0.809 & -0.264 & -1.538 & -0.800 & -0.599 \\ 1.127 & , & 1.048 & 0.698 & 0.460 & -0.071 & -1.257 & -1.415 & -0.590 \end{matrix}$   
 mean=0,0; stDev=1,1

thiel sen y-Intercept, slope = (9.06, 0.98)

SVD(Normalized X w/ dimension reduction):

$U =$   
 $\begin{matrix} -0.7071 & , & -0.7071 \\ -0.7071 & , & 0.7071 \end{matrix}$

$S = [3.6376280065322755, 0.8761635042000003]$

$V^T =$   
 $\begin{matrix} -0.3046, -0.5173, -0.2016, -0.2467, 0.0650, 0.5432, 0.4306, 0.2312 \\ 0.5543, -0.4565, 0.2890, -0.2812, 0.1561, 0.2269, -0.4959, 0.0073 \\ -0.3223, 0.0926, 0.9230, -0.0247, -0.0024, 0.0974, 0.1511, 0.0512 \\ -0.0266, -0.3895, 0.0568, 0.9071, 0.0454, 0.1042, -0.0902, 0.0215 \\ -0.0405, 0.1676, -0.0345, 0.0326, 0.9818, -0.0255, 0.0593, -0.0004 \\ 0.2859, 0.5470, -0.0318, 0.1659, -0.0702, 0.7613, 0.0287, -0.0728 \\ 0.6181, -0.1015, 0.1355, 0.0648, -0.0041, -0.2052, 0.7298, -0.1016 \\ 0.1734, 0.1621, 0.0077, 0.0618, -0.0230, -0.1037, -0.0265, 0.9632 \end{matrix}$

$U_0 * S_0 = [-2.572, -2.572]$

$U_1 * S_1 = [-0.620, 0.620]$

$A * V =$

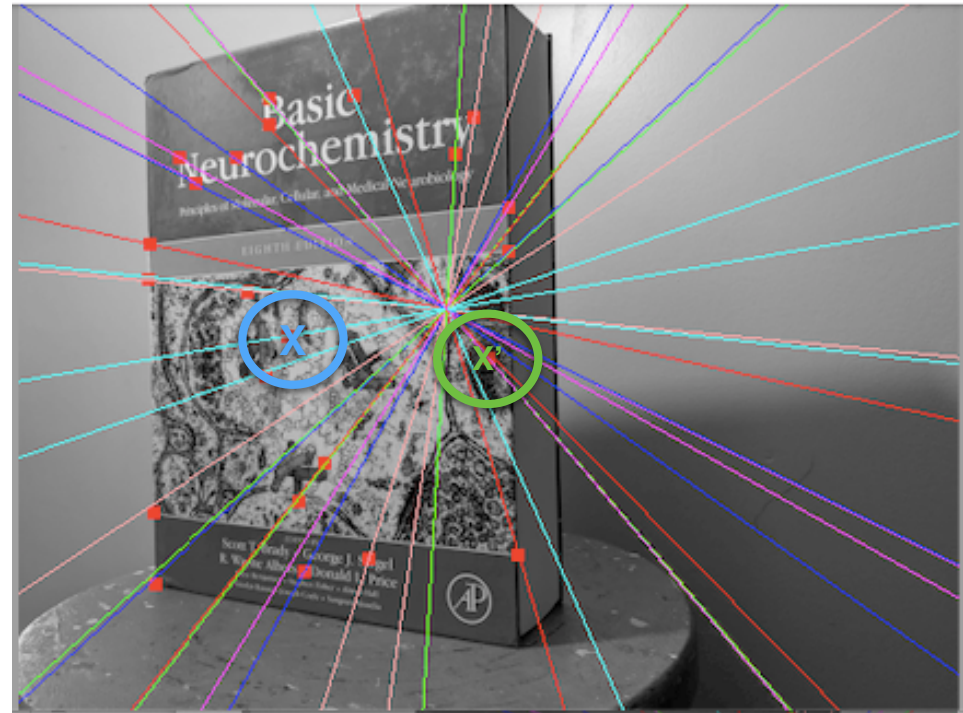
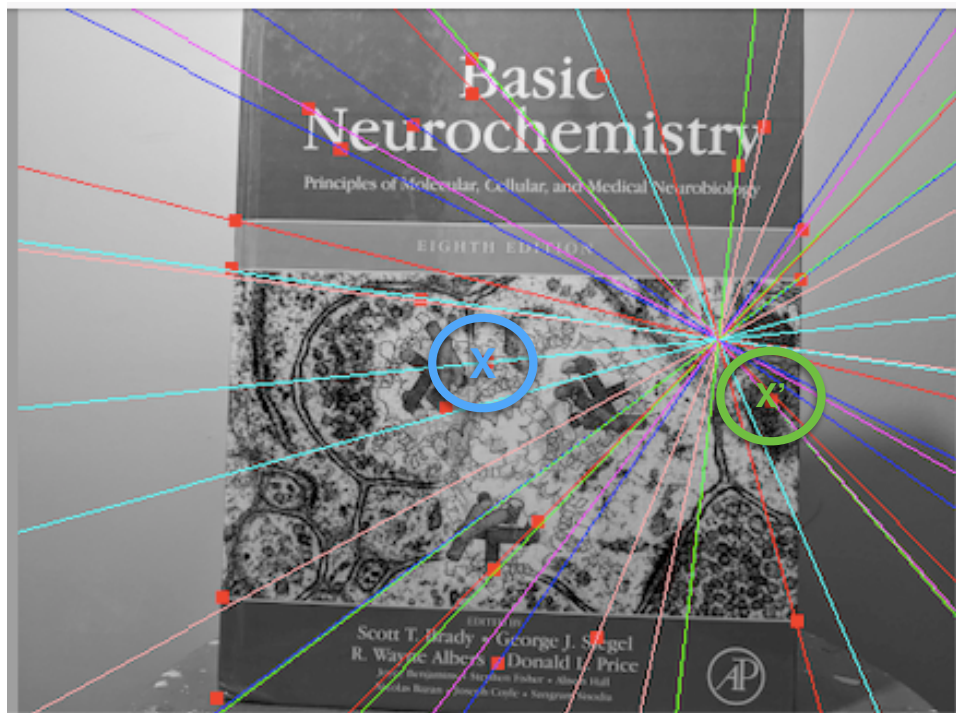
$\begin{matrix} -2.572 & , & -0.620 & 0.000 & -0.000 & 0.000 & -0.000 & -0.000 & -0.000 \\ -2.572 & , & 0.620 & -0.000 & -0.000 & -0.000 & 0.000 & -0.000 & 0.000 \end{matrix}$

$A * v_0 = [-2.572, -2.572]$

$a^T * u_0 = [-1.108, -1.882, -0.733, -0.897, 0.237, 1.976, 1.566, 0.841]$

$a^T * u_1 = [0.486, -0.400, 0.253, -0.246, 0.137, 0.199, -0.434, 0.006]$

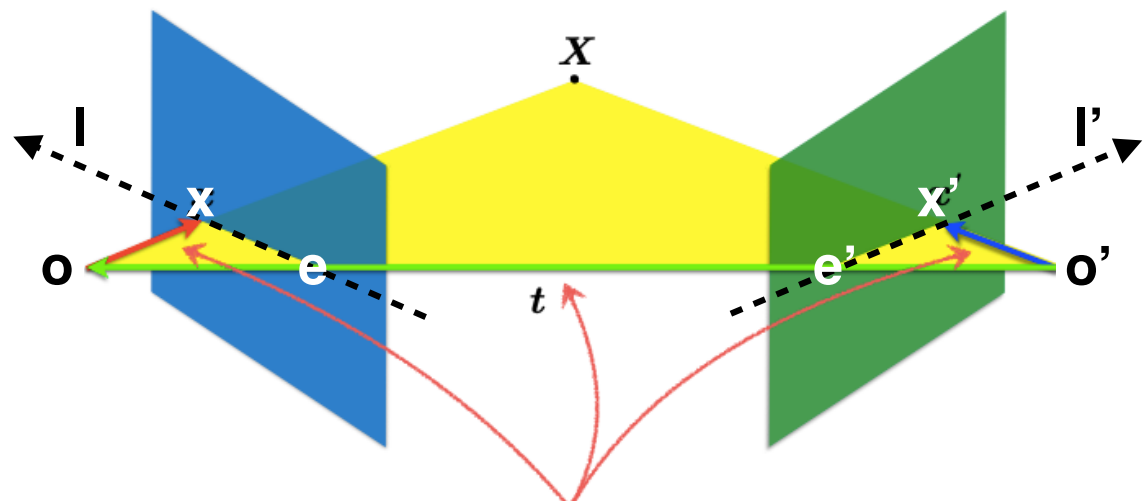
X



```
RANSAC fit=nMatchedPoints=24 nMaxMatchable=24  
tolerance=0.8033804327526433  
meanDistFromModel=2.210e-01 stDevFromMean=2.092e-01
```

```
de-normalized FM=  
2.573e-06, -5.055e-05, 8.106e-03  
4.471e-05, 2.159e-06, -1.748e-02  
-7.995e-03, 1.143e-02, 1.000e+00
```

```
P2=  
-4.626e-03, 6.614e-03, 5.786e-01, 8.157e-01  
6.522e-03, -9.325e-03, -8.156e-01, 5.785e-01  
3.498e-05, 3.100e-05, -1.894e-02, 3.498e-03
```



SVD and epipolar details on test images:  
RANSAC w/ **chirality filter**

SVD and epipolar details on test images

SVD and epipolar details on test images

## SVD and epipolar details on test images

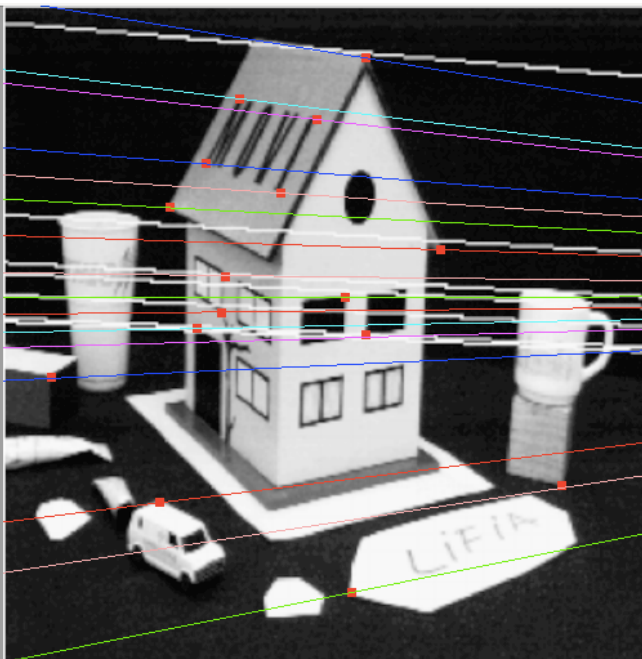
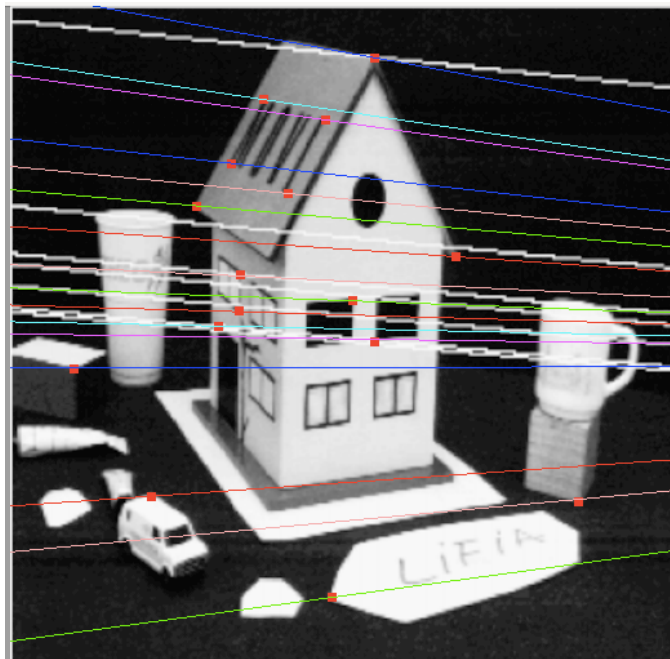
### In Defense of the Eight-Point Algorithm Richard I. Hartley

IEEE TRANSACTIONS ON PATTERN ANALYSIS AND MACHINE INTELLIGENCE, VOL. 19, NO. 6, JUNE 1997

To verify this conclusion, below is the fundamental matrix for the pair of house images in Fig 1.<sup>3</sup>

$$F = \begin{pmatrix} -9.796e-08 & 1.473e-06 & -6.660e-04 \\ -6.346e-07 & 1.049e-08 & 7.536e-03 \\ 9.107e-04 & -7.739e-03 & -2.364e-02 \end{pmatrix} \quad (7)$$

normalized by  $F[2][2]$ :  
 4.144e-06, -6.231e-05, 2.817e-02  
 2.684e-05, -4.437e-07, -3.188e-01  
 -3.852e-02, 3.274e-01, 1.000e+00



From this project's code: 16 points and their colored epipolar lines give similar sol'n to Hartley '97.

de-normalized FM=  
 4.135e-06, -1.065e-04, 2.302e-02  
 9.411e-05, 7.768e-06, -1.500e-01  
 -2.698e-02, 1.493e-01, 1.000e+00

## SVD and epipolar details on test images

### In Defense of the Eight-Point Algorithm Richard I. Hartley

IEEE TRANSACTIONS ON PATTERN ANALYSIS AND MACHINE INTELLIGENCE, VOL. 19, NO. 6, JUNE 1997

The normalized stats for the 16 correspondences:

```
fm before de-normalization FM=
-2.430e-03, -5.531e-02, 3.050e-02
6.257e-02, -4.565e-03, -7.036e-01
-3.560e-03, 7.049e-01, -2.492e-04

dist sampson^2=
 1.667e-04, 7.893e-04, 5.188e-04, 7.936e-04, 1.074e-03, 2.336e-03,
 9.733e-03, 2.382e-02, 5.401e-05, 7.407e-03, 9.218e-04, 8.365e-05,
 7.631e-04, 5.049e-05, 1.338e-03, 3.144e-03
dist perp to epipolar^2=
 6.674e-04, 3.157e-03, 2.075e-03, 3.174e-03, 4.298e-03, 9.342e-03,
 3.894e-02, 9.530e-02, 2.163e-04, 2.966e-02, 3.689e-03, 3.347e-04,
 3.053e-03, 2.019e-04, 5.353e-03, 1.258e-02
Total dist_sampson = 2.302e-01
Total dist_perp = 4.605e-01
```

The de-normalized stats for the 16 correspondences:

```
de-normalized FM=
4.135e-06, -1.065e-04, 2.302e-02
9.411e-05, 7.768e-06, -1.500e-01
-2.698e-02, 1.493e-01, 1.000e+00

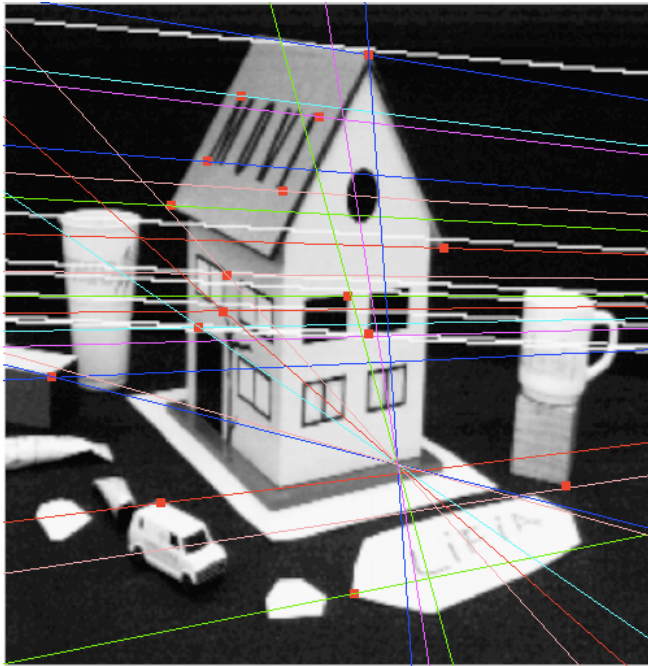
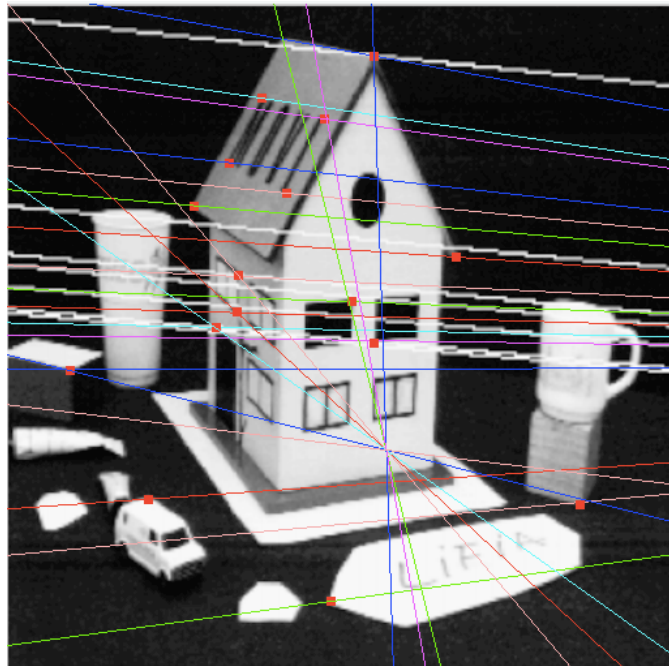
sampspon errors=nMatchedPoints=16 nMaxMatchable=16 tolerance=2.0
 meanDistFromModel = 3.848e-01 stDevFromMean=4.398e-01
 tol=2.0

epipolar fit=nMatchedPoints=14 nMaxMatchable=16 tolerance=2.0
 meanDistFromModel = 4.824e-01 stDevFromMean=4.257e-01
 tol=2.0
```

## SVD and epipolar details on test images

### In Defense of the Eight-Point Algorithm Richard I. Hartley

IEEE TRANSACTIONS ON PATTERN ANALYSIS AND MACHINE INTELLIGENCE, VOL. 19, NO. 6, JUNE 1997



From this project's code: 8 out of the 16 points and their colored epipolar lines give similar sol'n to Hartley '97.  
de-normalized FM=  
 $-1.867e-06, -1.522e-04, 5.262e-02$   
 $1.570e-04, 5.769e-06, -4.772e-02$   
 $-5.523e-02, 4.414e-02, 1.000e+00$

## SVD and epipolar details on test images

### In Defense of the Eight-Point Algorithm Richard I. Hartley

IEEE TRANSACTIONS ON PATTERN ANALYSIS AND MACHINE INTELLIGENCE, VOL. 19, NO. 6, JUNE 1997

The normalized stats for the 8 correspondences:

```
fm before de-normalization FM=
5.306e-03, -4.461e-01, 5.010e-01
4.327e-01, -1.640e-02, -3.059e-01
-4.370e-01, 2.779e-01, 1.306e-02

dist sampson^2=
3.691e-03, 5.770e-04, 8.350e-03, 1.686e-03, 3.993e-03, 1.151e-02,
1.313e-02, 2.375e-05
dist perp to epipolar^2=
1.485e-02, 2.325e-03, 3.411e-02, 6.791e-03, 1.602e-02, 4.712e-02,
5.255e-02, 9.731e-05
Total dist_sampson = 2.073e-01
Total dist_perp = 4.170e-01
```

The de-normalized stats for the 8 correspondences:

```
de-normalized FM=
4.135e-06, -1.065e-04, 2.302e-02
9.411e-05, 7.768e-06, -1.500e-01
-2.698e-02, 1.493e-01, 1.000e+00

sampspon errors=nMatchedPoints=6 nMaxMatchable=8 tolerance=2.0
meanDistFromModel = 4.841e-01 stDevFromMean=5.931e-01
tol=2.0
epipolar fit=nMatchedPoints=5 nMaxMatchable=8 tolerance=2.0
meanDistFromModel = 5.015e-01 stDevFromMean=3.390e-01
tol=2.0
```

SVD and epipolar details on test images

Using RANSAC on the Hartley 1997 house  
with the **cheirality filter**

SVD and epipolar details on test images

In Defense of the Eight-Point Algorithm Richard I. Hartley

IEEE TRANSACTIONS ON PATTERN ANALYSIS AND MACHINE INTELLIGENCE, VOL. 19, NO. 6, JUNE 1997

SVD and epipolar details on test images

In Defense of the Eight-Point Algorithm Richard I. Hartley

IEEE TRANSACTIONS ON PATTERN ANALYSIS AND MACHINE INTELLIGENCE, VOL. 19, NO. 6, JUNE 1997

The remaining notes and snapshots on corners, stereo matching and matching under conditions of different lighting, pose and location are in file **doc/colorSegmentation3.pdf**

**Note:** tried the use of a segmentation filter based upon the atrous wavelet to limit the points to be matched. (later methods of MSER + HOGs proved more successful).

